# The Robustness of Computer Vision Models against Common Corruptions: a Survey

Shunxin Wang, Raymond Veldhuis, Nicola Strisciuglio

**Abstract**—The performance of computer vision models are susceptible to unexpected changes in input images when deployed in real scenarios. These changes are referred to as common corruptions, and include illumination changes, blur, perspective transformations, etc. While they can hinder the applicability of computer vision models in real-world scenarios, they are not always considered as a testbed for model generalization and robustness. In this survey, we present a comprehensive and systematic overview of methods that improve the robustness of computer vision models against common corruptions. Unlike existing surveys that focus on adversarial attacks and label noise, we cover extensively the study of robustness to common corruptions that can occur when deploying computer vision models to work in practical applications. We describe different types of image corruption and provide the definition of corruption robustness. We then introduce relevant evaluation metrics and benchmark datasets. We categorize methods into four groups based on the part of the models and training method they address: data augmentation, knowledge distillation, robust representation learning, and robust network layers. We also cover indirect methods that show improvements in generalization and may improve corruption robustness as a byproduct. We report benchmark results collected from the literature and find that they are not evaluated in a unified manner, making it difficult to compare and analyze. We thus built a unified benchmark framework to obtain directly comparable results on several datasets containing a wide range of corruptions (ImageNet-C, ImageNet-$\bar{\text{C}}$, ImageNet-3DCC, and ImageNet-P). Furthermore, we evaluate relevant backbone networks pre-trained on ImageNet using the developed framework, providing an overview of the base corruption robustness of existing models to help choose appropriate backbones for computer vision tasks. Based on the comparison and analysis of relevant methods and backbones, we identify that developing methods to handle a wide range of corruptions and efficiently learn with limited data and computational resources is crucial for future development in the field of computer vision. Additionally, we highlight the need for further investigation into the relationship among corruption robustness, OOD generalization, and shortcut learning.

**Index Terms**—Robustness, common corruptions, computer vision

◆

## 1 INTRODUCTION

### 1.1 Background and motivation

OVER the past decade, deep neural networks (DNNs) have been applied widely in many fields, such as face verification (e.g. banking [1], criminal tracking [2], boarder control [3]), autonomous driving [4], medical imaging [5] and computer-aided diagnoses [6], education [7, 8], recommender systems [9], camera-based product quality monitoring [10], among others. In computer vision, DNNs are a core component of hallmark tasks such as object recognition [11], object detection [12], segmentation [13], image captioning [14], image super-resolution [15], image reconstruction [16], image generation [17], image retrieval [18], among others.

DNNs experience performance degradation in case of data distribution shifts, where the characteristics of test datasets differ from those of the training data [19]. For instance, a DNN-based medical diagnosis model trained on images captured from one hospital may not provide accurate diagnoses when applied to images from another hospital [20]. A doctor can instead make diagnoses based on images captured in different hospitals. This phenomenon becomes evident when DNNs trained on and that achieve high results on benchmark datasets are applied to real-world tasks. The observed degradation of performance poses a question about the reliability of DNNs [21]. This aspect is not always considered in experimental evaluations

and contrasts with what is experienced with the human visual system which appears to be more robust in handling unexpected or unknown cases [22].

Studies on the robustness of DNNs for image classification have revealed that their performance is affected by three main factors, namely label noise [23], shortcut learning [24], and data distribution shifts [19].

Label noise occurs when an image is mislabeled in the ground truth. This negatively affects the effectiveness of the models [25, 26, 27], as the incorrect label information provides confounding inputs to the DNNs during training [28, 29]. DNNs may overfit the label noise and consequently perform erroneous predictions [26].

Shortcut learning refers to the behavior of DNNs that exploit simple solutions in the data instead of learning task-related semantic solutions. This might negatively impact the performance of models when tested on new, unseen data [24]. An example of shortcut learning is shown in Fig. 1a, where a text is embedded in images of a certain class [30]. The presence of the text in images of other classes leads to incorrect predictions because a model has learned the text to be the defining feature of that class. Shortcut learning harms the robustness of DNNs since the spurious correlations between images and ground truth labels may be misused as a backdoor, e.g. manually embedding the shortcut features of a certain class to other classes results in false predictions.
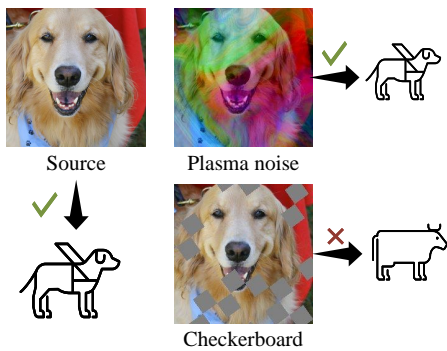
Data distribution shifts can take various forms, e.g.
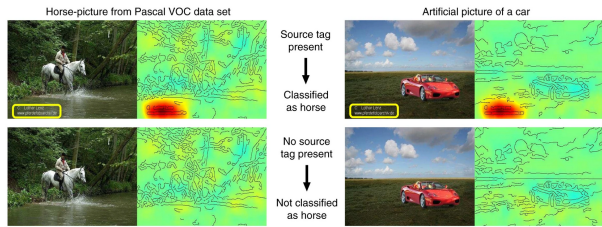
(a) Text embedded in training images of class 'horse' forms a spurious correlation between class 'horse' and the text, leading to incorrect predictions when the text is embedded in an image of a car [30].
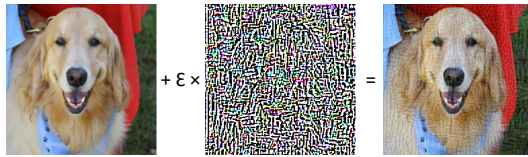


(b) Adversarial noise



(c) A clean image and an image corrupted with plasma noise can be correctly classified as class 'dog' by NNs while an image corrupted with checkerboard may be incorrectly predicted as 'cow'.

Fig. 1: Examples of (a) shortcut learning, (b) adversarial noise, and (c) common corruptions of plasma noise and checkerboard effect.

adversarial noise [31] and common image corruptions [32]. Adversarial noise is visually imperceptible noise embedded in an image that impairs classification performance [31]. Common image corruptions are caused by distortions like noise, blur, or digital transformation that can occur during image collection or transmission [32]. Examples of adversarial noise and common image corruptions are shown in Figs. 1b and 1c, respectively. Adversarial noise and image corruptions can cause significant performance degradation in computer vision models, and it has become an increasingly popular research topic [33, 34, 35, 36, 37, 38, 39] to improve model robustness to common corruptions (see Fig. 2).

## 1.2 Terminology

**Image corruptions** *are visible distortions applied to images, causing a shift in data distribution from that of the original training data.* Thus, they are a type of data distribution shift. Common image corruptions in real scenarios include Gaussian noise, impulse noise, defocus blur, etc. Weather conditions also affect image quality, due to the presence of
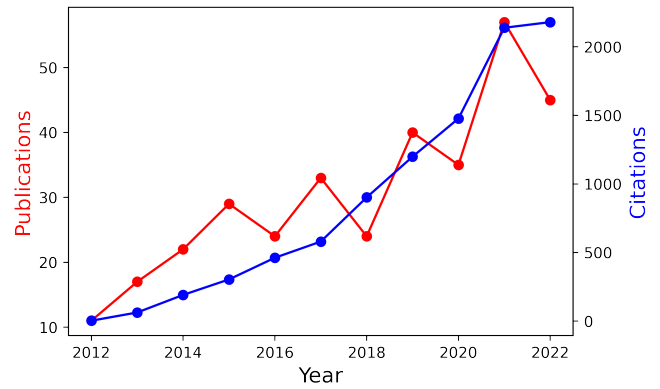


Fig. 2: The number of related publications to robustness to common image corruptions and the corresponding citation numbers from the year 2012 to 2022 (searched with keywords: 'image corruption', 'corruption robustness', 'robustness to corruption' and generated from Web of Science).

fog, snow, etc. Examples of common corruptions are shown in Figs. 3b to 3e, which are chosen from the ImageNet-C [32], ImageNet-C̄ [40], ImageNet-3DCC [41], and Continuously Changing Corruptions (CCC) [42] datasets. Different from adversarial noise, image corruptions are visible transformations in images.

**Corruption robustness** *refers to the ability of a computer vision model to withstand image corruptions that are unexpected and may occur in the test samples without significant degradation of performance.* High corruption robustness means small performance degradation under image corruptions, to which the models generalize well. Note that the corruptions being tested should not be used for training, to ensure unbiased evaluation [32].

## 1.3 Contributions

We present a survey of research focused on improving the robustness of computer vision models to common corruptions that may be encountered when deploying systems in real-world scenarios. We focus on the period between 2012 and 2023, during which significant progress has been made in this area. We collected benchmark results from relevant papers and found they are not measured in a unified way. Thus, we built a comprehensive benchmark suite for evaluating model performance on publicly available benchmarks. We then evaluate the robustness of popular ImageNet pretrained backbones to common corruptions and provide a comprehensive analysis. Our analysis includes unified comparisons of model performance. By surveying the latest research in this area, we aim to provide insights into effective approaches for improving the robustness of computer vision models against common corruptions and identify areas for future research. Ultimately, our goal is to contribute to the development of more robust and reliable computer vision systems that can operate effectively in real-world scenarios. To summarize, our contributions are as follows.

First, we present a comprehensive and systematic overview and taxonomy of works that characterize or improve the robustness of DNNs against common image cor-
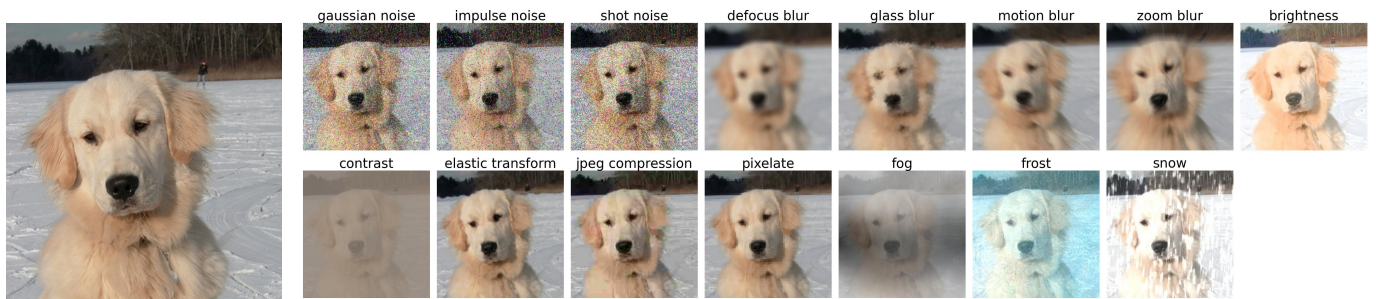
(a) Original image.

(b) Corruption types in ImageNet-C are grouped into four categories: noise, blur, digital transformation and weather [32].
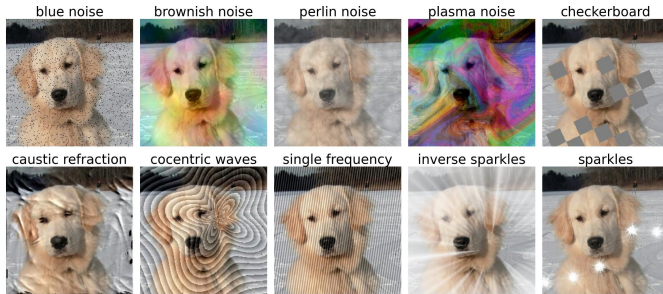
(c) Corruption types in ImageNet-C̄ are perceptually dissimilar to those in ImageNet-C, which increases the coverage of the benchmark for evaluating the corruption robustness of computer vision models [40].
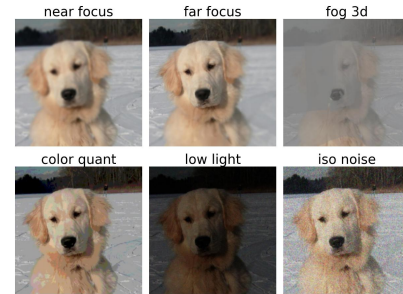
(d) Corruption types in ImageNet-**3DCC** use 3D information from real-world, improving the realness of the synthetic corruptions [41].
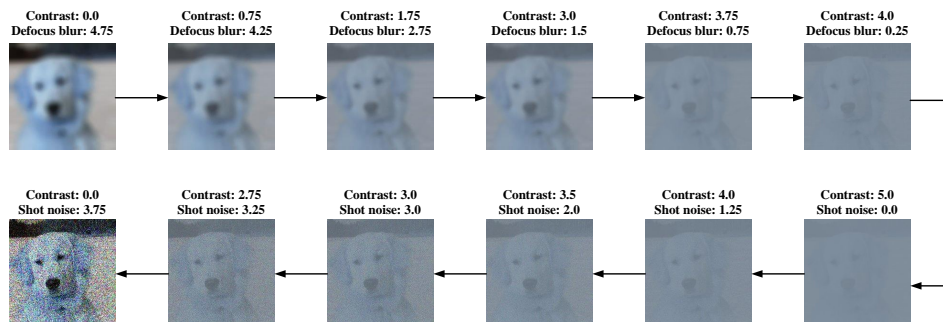
(e) Continuously Changing Corruptions (CCC) [42]. Random walk is used to find the combination of corruptions in an image.

Fig. 3: Examples of common corruptions in computer vision.

ruptions in computer vision. To the best of our knowledge, no other survey has focused on the corruption robustness of computer vision models, providing a systematic taxonomy of methods, and a uniform comparison and analysis of different approaches. We aim to fill this gap in the literature by presenting a comprehensive analysis of current research efforts, while Hendrycks *et al.* [32] instead provided benchmark metrics for evaluating corruption robustness. We categorize the methods for directly improving corruption robustness into four groups, namely: 1) data augmentation, 2) robust representation learning, 3) knowledge distillation, and 4) network layer modification. We review also methods for improving generalization performance w.r.t. Out-of-Distribution (OOD) data, which may also improve the corruption robustness of DNNs. We refer to these methods as indirect methods, and categorize them into four groups,

i.e. 1) image restoration, 2) regularization, 3) robust optimization, and 4) shortcut learning mitigation.

Second, we carried out an extensive benchmark of several relevant backbone networks for computer vision on benchmark datasets, namely ImageNet-C, ImageNet-C̄, ImageNet-3DCC, and ImageNet-P. We investigate the robustness of different backbones against common corruptions, studying the impact of the complexity of network architecture and model size. The efforts made in this work for the unification of benchmark results provide a solid ground to analyze the pros and cons of different methods and summarize current research tendencies. We further identify future research challenges and promising research directions related to improving corruption robustness. Finally, we contribute to making further steps toward the understanding of corruption robustness, generalization, and

shortcut learning in computer vision.

The remainder of this paper is organized as follows. In Section 2, we describe other survey papers that examine methods for improving the robustness of DNNs against adversarial attacks and label noise. In Section 3, we introduce benchmark datasets and evaluation metrics. In Section 4, we provide a taxonomy of methods designed to explicitly address corruption robustness. We present an overview of the results of these methods (collected from the papers) and investigate the corruption robustness of different relevant ImageNet pre-trained backbones (with a corruption robustness evaluation framework that we made publicly available) on benchmark datasets in Section 5. In Section 6, we introduce approaches that indirectly related to the robustness of computer vision models, and in Section 7, we discuss future challenges and opportunities for improving corruption robustness, followed by conclusions in Section 8.

## 2 RELATED WORKS

The survey papers about robust deep learning mostly focus on robustness against adversarial attacks and label noise [31, 43, 44, 23, 5, 45, 46, 47]. In this section, we provide an overview of these surveys and discuss the evolution of their taxonomy over time.

### 2.1 Adversarial attacks and defenses.

DNNs are known to be vulnerable to small, imperceptible perturbations of their inputs, called adversarial attacks, which can lead to subtle misclassification. To improve robustness against adversarial attacks, various defense methods have been developed, including gradient masking or obfuscation [48], adversarial training [49], regularization approaches [50] and adversarial example detection [51]. A comprehensive overview of different types of adversarial attacks and the corresponding defense methods was presented in [31]. The authors categorized adversarial attack scenarios based on (1) when an attack happens (during training, testing, and application), (2) the prior knowledge of the target model (white-box or black-box attacks), and (3) the target of the attack (prediction confidence reduction, targeted or non-targeted misclassification). They further discussed defense methods and grouped them based on the way of implementation, including adversarial training, gradient hiding, defensive distillation, and feature squeezing. In [43], the authors further extended the categorizations of defense methods based on the work presented in [31], including gradient masking/obfuscation, robust optimization, and adversarial example detection. They mainly focused on methods for robust optimization including adversarial training, certified defenses, and regularization approaches. Different from model-agnostic common image corruptions, the generation of adversarial noise depends on the knowledge of a specific model. In [52], adversarial noise was shown to have a beneficial effect on the robustness of DNNs to common image corruptions.

### 2.2 Label noise

Label noise refers to the presence of incorrect ground truth labels that can mislead the training of DNNs, resulting in suboptimal model performance. The existence of label noise is hard to avoid since many datasets are labeled by non-experts or in a crowd-sourcing manner [53, 54]. Additionally, some data contains ambiguous information, making it difficult even for experts to annotate correctly. The practice of training models on large-scale annotated datasets often involves the dependency on non-expert annotators (crowd-sourced labeling) [55] or pseudo labels created by the training models [56] to reduce the expensive cost of annotation. These approaches result in an increase of label noise [57]. Noisy labels are hard to recognize during training, and approaches to detect label noise and remove its influence are essential to improve the classification performance and robustness of DNNs. A taxonomy of label noise and its influence on the training of deep neural networks was presented in [23]. Different types of label noise were identified based on their statistical characteristics, i.e. the dependency on other variables such as the characteristics of certain classes. Label noise can have a significant impact on various aspects of a DNN, including classification performance, learning requirements, and model complexity and capacity. The methods reviewed in [5] to learn with label noise were grouped by implementation principles (e.g. ground truth label estimation and direct learning with label noise). New categories of robust methods against label noise were introduced in [45] (i.e. loss function and sample selection) and in [46] (i.e. sample weighting and meta-learning). The authors of [58] categorized the methods from a wider perspective (e.g. data modification, objective function, and optimization) than the previous surveys, and the categorization was further extended in [47] with extra groups like regularization and architecture modification.

These works presented an overview of methods for improving robustness toward adversarial attacks and label noise. However, an overview of methods for improving the robustness of computer vision models toward common image corruptions, with a unified analysis of their performance, is not yet available.

## 3 DATASETS AND METRICS

In this section, we introduce existing benchmark datasets to evaluate corruption robustness, adversarial robustness, and OOD generalization, followed by relevant evaluation metrics.

### 3.1 Benchmark datasets for corruption robustness

Two benchmark datasets to evaluate and compare the corruption robustness, CIFAR-C and ImageNet-C, were proposed in [32]. The datasets were generated from the validation set of CIFAR-10/100 and ImageNet respectively. CIFAR-C contains 19 synthetic corruptions while ImageNet-C contains 15 corruptions. There are four extra corruptions for ImageNet-C, which serve as a simplified corruption robustness validation set. Each corruption has five levels of severity. High severity indicates high strength of corruption applied to the source images. Fig. 3b shows the corruption types proposed in [32] with severity level equals to three.

The corruption types in CIFAR10-C and ImageNet-C are insufficient to represent all the possible variations that

can occur in the real world. Two complementary datasets, CIFAR-$\bar{\text{C}}$ and ImageNet-$\bar{\text{C}}$ were thus designed [40]. The set of corruptions included in these datasets contains the 10 most perceptually dissimilar corruptions to those of CIFAR-C and ImageNet-C (see Fig. 3c). To ensure realness, ImageNet-3DCC was designed, consisting of images generated by 3D corruptions that consider the scene geometry (see Fig. 3d) [41]. Thus, the resulting corruptions are more consistent with what may occur in the real world. For more data variety, Continuously Changing Corruptions (CCC) [42] combines pairs of corruptions to generate the corrupted images. As shown in Fig. 3e, corruption types of varying severity and characteristics are combined through random walks to create a diverse set of benchmarks. To inspect how model predictions change as the effect of corruptions varies over time, time-dependent perturbation sequences were generated in the CIFAR-P and ImageNet-P datasets [32]. Each frame of a sequence is perturbed based on its previous frame.

Although benchmark datasets are synthetically generated and may not cover all possible variations of corruptions that might occur in real-world scenarios, they still offer extensive ground for comparing the robustness of computer vision models. These datasets contain a wide range of corruption types, enabling the assessment of different aspects of robustness and generalization that are not typically evaluated when testing new algorithms and models. We thus contend that incorporating robustness testing into the performance evaluation of computer vision models should be a standard practice.

## 3.2 Benchmark datasets for adversarial robustness and OOD generalization

Adversarial robustness is also an essential aspect to assess computer vision models. In [62], two benchmark datasets named ImageNet-A and ImageNet-O were proposed. Both datasets contain naturally occurring adversarial images which are hard to recognize. ImageNet-O contains images of unknown classes while ImageNet-A contains images of known classes (seen during training). In [63], the authors proposed ImageNet-Patch, where an image contains adversarial patches that lead to degraded performance.

Examples of common OOD datasets are OOD-CV [64], SI-Score [65], and WILDS [66]. They contain variations like pose, shape, texture, context, location, size, rotation, etc. Images with different renditions from the training data are considered OOD data as well. Typical datasets are ImageNet-R [61], ImageNet-D [59], ImageNet-Cartoon [60], and ImageNet-Drawing [60]. These datasets allow for measuring the generalization performance of models to different abstract renderings and the dependence of models on natural textures. We report an overview of benchmark datasets for corruption robustness, adversarial robustness, and OOD generalization in Table 1, which includes detailed descriptions, e.g. the corruption types or rendition types of each benchmark dataset.

## 3.3 Evaluation metrics

### 3.3.1 Mean corruption and relative mean corruption error

Several evaluation metrics to measure corruption robustness were proposed in [32]. The mean corruption error (mCE) and relative corruption error (rCE) are basic metrics, computed as:

$$\text{mCE} = \frac{1}{|C|} \sum_{c \in C} \frac{\sum_{s=1}^{5} E_{s,c}^f}{\sum_{s=1}^{5} E_{s,c}^{baseline}}, \qquad (1)$$

and

$$\text{rCE} = \frac{1}{|C|} \sum_{c \in C} \frac{\sum_{s=1}^{5}(E_{s,c}^f - E_{clean}^f)}{\sum_{s=1}^{5}(E_{s,c}^{baseline} - E_{clean}^{baseline})}, \qquad (2)$$

where $E_{s,c}^f$ is the classification error rate of a tested model $f$ for a type of corruption $c$ with severity $s$ ranging from one to five, $C$ is the set of corruptions in the test set and $baseline$ indicates the baseline model used for comparison. The mCE measures the classification performance of a model with respect to that of the baseline over all types of image corruption in the considered test dataset. When mCE is larger than one, it indicates that the model $f$ is less robust than the baseline model, and vice versa. The rCE measures the performance degradation of model $f$ on corrupted images w.r.t. their source images, and compares it with that of the baseline model. Thus, a low rCE value indicates better corruption robustness of the tested model, compared to the baseline model.

### 3.3.2 Mean flip rate

Mean flip rate (mFR) [32] was designed for the evaluation of the effects that consecutive corruptions have on the classification performance of models over time. It evaluates the probability of models changing their prediction across consecutive frames [32]. It is specifically used for image sequences having the same structure as those in ImageNet-P, where each sequence contains frames that are corrupted using the same type and level of corruption on top of the previous frame. The Flip Probability (FP) of the tested model $f$ for the perturbation $p$ is computed as:

$$\text{FP}_p^f = \frac{1}{m(n-1)} \sum_{i=1}^{m} \sum_{j=2}^{n} \mathbb{1}(f(x_j^{(i)}) \neq f(x_{j-1}^{(i)})), \qquad (3)$$

where $m$ is the number of perturbation sequences, $n$ is the number of frames in a sequence, $x^{(i)}$ indicates the $i^{th}$ sequence in the dataset and $x_j$ indicates the $j^{th}$ frame of a sequence. $\sum_{j=2}^{n} \mathbb{1}(f(x_j^{(i)}) \neq f(x_{j-1}^{(i)}))$ measures the number of frames in a sequence having different predictions from their previous frame. It compares the prediction of the model $f$ on the a frame $x_j$ of the $i^{th}$ sequence with that on the previous perturbed images in the sequence. If the predictions are the same, $\mathbb{1}(f(x_j^{(i)}) \neq f(x_{j-1}^{(i)}))$ equals to zero, and the performance of the model is not affected by the considered perturbations. For a sequence corrupted by noise, the predictions are compared with those of the first frame, as noise is not temporally related. The mFR is obtained by averaging the flip rate $\text{FR}_p^f$ across all the perturbations:

$$\text{mFR} = \frac{1}{|P|} \sum_{p \in P} \text{FR}_p^f = \frac{1}{|P|} \sum_{p \in P} \frac{\text{FP}_p^f}{\text{FP}_p^{baseline}}, \qquad (4)$$

TABLE 1: Benchmark datasets for data distribution shifts such as corruption, adversarial noise, rendition

| Category | Dataset | Image variation types |
|---|---|---|
| corruption | CIFAR-C [32] | Noise (Gaussian, Impulse, Shot, Speckle)<br>Blur (Defocus, Glass, Gaussian, Motion, Zoom )<br>Weather (Fog, Frost, Snow, Spatter)<br>Digital Transformation (Brightness, Contrast, Elastic, Jpeg compression, Pixelate, Saturate) |
| | ImageNet-C [32] | Noise (Gaussian, Shot, Impulse)<br>Blur (Defocus, Frosted glass, Motion, Zoom)<br>Weather (Snow, Frost, Fog)<br>Digital Transformation (Brightness, Contrast, Elastic, Pixelate, JPEG) |
| | CIFAR-$\bar{\text{C}}$ [40] | Noise (Brown, Blue)<br>Blur (Circular Motion Blur, Transverse Chromatic Aberration )<br>Digital transform (Checkerboard, Lines, Inverse Sparkle, Sparkles, Pinch and Twirl, Ripple) |
| | ImageNet-$\bar{\text{C}}$ [40] | Noise(Brown, Perlin, Blue, Plasma, Single Frequency, Concentric Sin Waves)<br>Digital transform (Checkerboard, Caustic Refraction, Inverse Sparkle, Sparkles) |
| | CIFAR-P [32] | Noise (Gaussian, Shot)<br>Blur (Motion, Zoom )<br>Weather (Snow)<br>Digital Transformation (Brightness, Rotate, Scale, Tilt, Translate) |
| | ImageNet-P [32] | Noise (Gaussian, Impulse, Shot, Speckle)<br>Blur (Defocus, Glass, Gaussian, Motion, Zoom )<br>Weather (Fog, Frost, Snow, Spatter)<br>Digital Transformation (Brightness, Contrast, Elastic, Jpeg compression, Pixelate, Saturate) |
| | ImageNet-3DCC [41] | Noise (ISO, Low-light)<br>Blur (Far focus, Near focus, XY-Motion, Z-Motion)<br>Weather (Fog 3D, Shadow, Multi-illumination, )<br>Digital Transformation (Occlusion, Scale, Bit Error, Color Quantization, Flash, CRF Compress, Camera Pitch, Camera Roll, Field of View, View Jitter, ABR Compress) |
| | CCC [42] | Noise (Gaussian, Impulse, Shot, Speckle)<br>Blur (Defocus, Glass, Gaussian, Motion, Zoom )<br>Weather (Fog, Frost, Snow, Spatter)<br>Digital Transformation (Brightness, Contrast, Elastic, Jpeg compression, Pixelate, Saturate) (*Appied in random pairs.*) |
| rendition | ImageNet-D [59] | Real, Painting, Clipart, Sketch, Infograph and Quickdraw |
| | ImageNet-Cartoon [60] | ImageNet images converted to cartoon style |
| | ImageNet-Drawing [60] | ImageNet images converted to colored pencil drawings |
| | ImageNet-R [61] | Art, Cartoon, Graffiti, Line Drawing, Graphics, Origami, Painting, Pattern, Tattoo, Plastic Object, Plush Object, Video Game, Sculpture, Toy, and Embroidery |
| adversarial | ImageNet-A [62] | Adversarial noise exists in the collected samples |
| | ImageNet-O [62] | Adversarial noise exists in the collected samples |
| | ImageNet-Patch [63] | Adversarial patch |
| OOD | OOD-CV [64] | Shape, 3D pose, Texture, Context, and Weather |
| | SI-Score [65] | Shifted object size, Location, and Angle. |
| | WILDS [66] | Composed of 10 datasets with different modalities and sizes |

where $P$ is the set of perturbations and $\text{FR}_p^f$ is the standardized flip probability of the model $f$ compared to that of the baseline model. The value of mFR is expected to be close to zero for a robust model.

### 3.3.3 Mean top-5 distance

Mean top-5 distance (mT5D) is also designed for ImageNet-P [32]. If a model is robust to the added perturbations, then the top-5 predictions of frames over a sequence should not be shuffled and should be relevant to those of the previous frames in the sequence. If the top-5 predictions are shuffled and inconsistent with those of the previous frames in a sequence, the model should be penalized for its lack of robustness in maintaining accurate predictions under the perturbations added in sequential order. The top-5 distance over each frame of $m$ sequences belonging to a perturbation is:

$$\text{T5D}_p^f = \frac{1}{m(n-1)} \sum_{i=1}^{m} \sum_{j=2}^{n} d(\tau(x_j), \tau(x_{j-1})), \quad (5)$$

where $d(\tau(x_j), \tau(x_{j-1}))$ measure the deviation between the top-5 predictions of two consecutive frames, using:

$$d(\tau(x_j), \tau(x_{j-1})) = \sum_{i=1}^{5} \sum_{j=min\{i,\rho(i)\}+1}^{max\{i,\rho(i)\}} \mathbb{1}(1 \leq j-1 \leq 5), \quad (6)$$

with

$$\rho(\tau(x_j)(k)) = \tau(x_{j-1})(k), \quad (7)$$

where $\tau(x_j)$ is the ranking of predictions for a perturbed frame $x_j$ and $\tau(x_j)(k)$ indicates the rank of the prediction being $k$. If $\tau(x_j)$ and $\tau(x_{j-1})$ are identical, then $d(\tau(x_j), \tau(x_{j-1})) = 0$. Averaging the normalized T5D (compared with the baseline model) of all the perturbations, the mT5D is:

$$\text{mT5D} = \frac{1}{|P|} \sum_{p \in P} \frac{\text{T5D}_p^f}{\text{T5D}_p^{baseline}}. \quad (8)$$

### 3.3.4 Relative robustness and effective robustness

While $\mathrm{mCE}$ and $\mathrm{rCE}$ directly evaluate the corruption robustness, other metrics are designed to measure the OOD performance of DNNs and may indirectly reveal the corruption robustness of models. The *Relative Robustness* $\phi(f')$ [67] was proposed to compare directly the accuracy $acc$ of a tested models $f'$ with the baseline model $f$ on the same dataset, computed as:

$$\phi(f') = acc_{dataset}(f') - acc_{dataset}(f). \tag{9}$$

A model with good relative robustness is expected to have a positive and high value of $\phi(f')$. The *Effective Robustness* $\epsilon(f')$ [67] was developed to compare the accuracy of a model tested on two different datasets, using:

$$\epsilon(f') = acc_{dataset_2}(f') - \beta(acc_{dataset_1}(f')), \tag{10}$$

where $\beta$ is a function approximating the performance of different baseline models. It was empirically shown that the performance of the baseline models with different architectures on the original test set and the distribution-shifted test set (corresponding to $dataset_1$ and $dataset_2$) fits a linear function. A positive high value of $\epsilon(f')$ indicates the model $f'$ is more robust than the baseline model on $dataset_2$. However, this metric is impacted by the selection and training of the baseline models, bringing uncertainty to the evaluation process.

### 3.3.5 Expected calibration error

Instead of comparing models with a baseline, expected calibration error (ECE) [68] compares the accuracy and the confidence of the predictions, examining whether the models give reliable predictions. It is computed as:

$$ECE = \sum_{m=1}^{M} \frac{|B_m|}{n} |acc(B_m) - conf(B_m)|, \tag{11}$$

where $M$ is the number of confidence interval bins separating the predictions, $B_M$ is the samples in a confidence interval bin, $n$ is the total number of samples in the test set, $acc(B_m)$ is the test accuracy of the set of samples $B_M$ while $conf(B_m)$ is the average confidence of the corresponding predictions. The lower the ECE, the more reliable the predictions.

## 4 A TAXONOMY OF METHODS ACHIEVING COR-RUPTION ROBUSTNESS

We present a systematic overview of existing methods to improve corruption robustness and categorize them into four groups based on the part of the models considered and training methods. These categories include 1) data augmentation, 2) robust representation learning, 3) knowledge distillation, and 4) robust network layer. The taxonomy of the methods is shown in Fig. 4. Since image corruption will cause data distribution shifts, we also consider methods addressing OOD generalization, as they might indirectly improve corruption robustness as a byproduct. Methods addressing OOD generalization mostly do not take corruption robustness into account in the performance evaluation process, but provide interesting ideas and insights that might inspire future works and strategies to unify robustness and
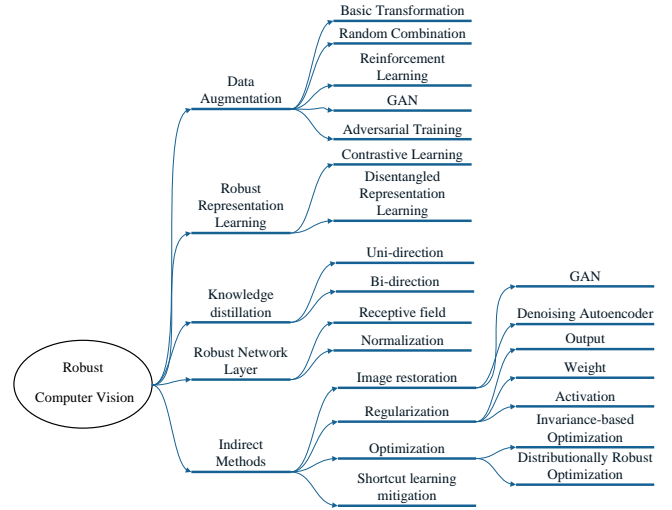


Fig. 4: Taxonomy of methods improving corruption robustness directly and indirectly.

generalization in computer vision. To differentiate from the methods targeting directly corruption robustness, we discuss the indirect approaches into four groups in Section 6.

### 4.1 Data Augmentation

Recent evidence suggests that the robustness of DNNs benefits enormously from well-annotated large-scale datasets since they contain more variations that might occur in the real world, filling the distribution gap between the training and unseen data [69, 67]. However, the cost of obtaining a large, well-annotated dataset can be excessively high. Thus, researchers synthetically generate data with different augmentations to increase data variety, bridging the distribution gap between training and testing data [38, 70]. This is shown to improve the corruption robustness of computer vision models [70].

*Basic data augmentations.* Basic data augmentation for image processing consists of simple transformations such as flipping, cropping, rotating, translation, color jittering, edge enhancement, etc [71]. Kernel filters are used to blur images, mimicking motion blur, defocus blur, among others [72]. Pixel erasing removes pixels randomly from images [73], which is inspired by dropout regularization. Instead of augmenting an entire image, Patch Gaussian augmentation [74] applies Gaussian noise to small patches of images, which benefits the classification performance on both clean images and those affected by common image corruptions.

*Advanced data augmentations.* Combining different transformations can better increase data variety. Mixup [75] generates images by interpolating linearly two source images. The corresponding ground truth label of the interpolated images is also interpolated from the ground truth of the two images. Thus, a model is trained to predict linearly based on the weight of each source image in the interpolated versions, which improves robustness to label noise and adversarial samples. As an extension of Mixup, RobustMix [76] fuses the frequency bands of two images. The weight of each frequency band depends on its relative amount of energy.

Color
Equalize
Invert
⋮
Sharpness
ShearX
Solarize
Posterize
Rotate

Augmentation
Candidate pool

Selection and
combination

Random

Adversarial

Policy-based

Augmented images by:
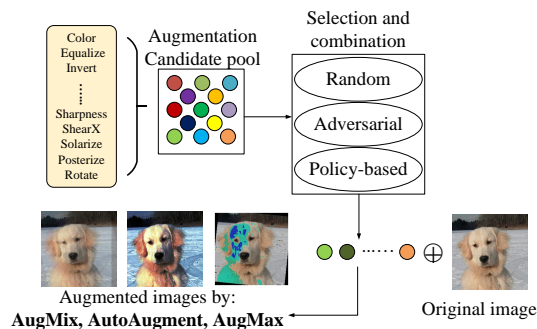**AugMix, AutoAugment, AugMax**

Original image

Fig. 5: Conceptual plot of automatic augmentation techniques. The selection and combination of the augmentations can be random, adversarial selected or based on learned policy.

Thus, the models are regularized to classify based on low-frequency spatial features, which are more robust than high-frequency features [77], as the models depend more on the shapes rather than textures for classification [78].

LISA [79] aims at learning invariant predictors through selective augmentation, i.e. intra-label and intra-domain augmentations. Intra-label augmentation interpolates samples with the same labels but in different domains, learning useful semantics rather than spurious relations between domain information and the ground truth labels. Intra-domain augmentation instead interpolates samples with different labels but in the same domain. The learned representations can ignore unrelated domain information and focus on discriminative information to distinguish the samples.

Reinforcement learning was utilized in [80] to search for the best combination of augmentations, with a method called AutoAugment. However, the search process is computationally intensive and dataset-specific. AugMix [38] augments images by randomly selecting augmentation operations. Jensen-Shannon divergence is applied to enforce the consistency of the augmented images (compared with the source image). Further, AugSVF [81] expands the options of possible transformations with additive Fourier-basis noise. Rather than randomly combining different augmentations, AugMax [82] adversarially selects augmentations and calculates the combined weights with back-propagation. PRIME [83] selects maximum-entropy image transformation, where the distributions of the chosen image transformations have maximum entropy. This guarantees that the complexity of samples reaches certain generalization bounds. Kim *et al.* [84] applied augmentations during test-time, which are selected by an auxiliary model that predicts suitable augmentations with low loss values. We provide a conceptual scheme of these automatic augmentation techniques in Fig. 5.

Targeted augmentation [85] is based on copy-paste, i.e. the object to be recognized is copied and pasted to different backgrounds, thus the predictive features that may vary across different backgrounds (domains) are preserved in the augmented images. This improves the generalization of models to OOD data, as it avoids learning the spurious correlation between backgrounds and the ground truth labels.

*Generative models.* The above augmentations manipulate images directly. Augmentations can also be achieved by deep learning models, such as generative adversarial neural networks (GANs) [86, 87, 88, 89] and variational autoencoders (VAEs) [90]. Inspired by style transfer, where different augmentations can be considered as different domains, CycleGAN [89] utilizes a pair of autoencoders for bidirectional mapping, i.e. transferring an image from one domain to another. The cycle consistency loss ensures that images mapped back to the source domain are not contradictory to the source images, thus improving the quality of the generated images. It was used in [91, 92] to perform data augmentation on medical images. Currently, DNN-based image generators aim at reducing data imbalance instead of improving corruption robustness. Although GANs and VAEs can generate an unlimited number of images with various levels of augmentation, the training process needs numerous computational resources and has high requirements of training data, when compared with basic augmentations. Moreover, the realness of the generated images needs more consideration, as it might affect the quality of training data.

*Adversarial training.* Adversarial training forces computer vision models to classify images with (imperceptible) adversarial noise correctly [93]. Originally, it aimed at improving the adversarial robustness of computer vision models [94]. Subsequently, models trained adversarially are found to be as robust as biological neurons to adversarial perturbations [95], and adversarial training can help improve the robustness of models to common image corruptions [52, 96]. Gaussian adversarial training (GAT) [93] enforces Gaussian distribution regularization to adversarial noise, which shows the feasibility of adversarial training in improving corruption robustness. A regularization term based on maximum entropy formulation is proposed in [97]. It encourages perturbing the source distribution of data rather than on the data directly. Thus, the generated adversarial samples bring more uncertainty to predictions. Rather than directly adding noise to input, adversarial noise propagation (ANP) focuses on injecting noise to the hidden layers of NNs, which can be easily combined with other adversarial training methods [98]. Similarly, NoisyMix [99] applies augmentations in both input and feature space, making the decision boundary smoother. Diverse augmentation-based joint adversarial training (DAJAT) [100] further combines adversarial training with common augmentations, where two models are trained with augmented images and their source images respectively. The models share the same weights but with different statistics for batch normalization layers, being more robust to distribution shifts.

The commonality of these approaches is the target to improve corruption robustness by reducing the distribution difference between training and testing data, as the synthetically generated images increase data variety.

### 4.2 Representation learning

Robust representation learning aims at learning representations that are invariant to non-semantic changes in input images. Common ways to achieve this are contrastive learning [101, 102] and disentanglement learning [103]. They share the same idea to learn invariant semantics irrelevant to domain information by enforcing models to ignore

domain-specific information. This can improve corruption robustness as the models learn to ignore the influence of corruptions.

*Contrastive learning.* Self-supervised learning is shown to be beneficial to improve the robustness of computer vision models [59, 104]. For instance, self-supervised contrastive learning [105] forces a model to learn similar latent representations for source images and their augmented versions, inducing the learning of representations that are invariant to non-semantic changes. This improves the robustness of the model when the learned representations are used for downstream tasks like classification. In contrastive learning, the images augmented from the same source image are called positive samples, while the rest are negative samples. The latent representations of the positive pairs are pulled together and the negative samples are pushed away from the positive samples (see Fig. 6). The authors in [106] use a perceptual similarity metric that mitigates the impact of irrelevant features on downstream tasks. The work in [107] combines adversarial training with contrastive learning. The problem with these methods is that the latent representations of the same class are also far away from each other, potentially influencing classification tasks, which need class-wise clustered representations. To avoid this, The authors of [108] additionally use k-means to generate pseudo labels, which are then used to group images with different pseudo labels into the same batch during training.

Supervised contrastive learning (SupCon) [102] forces the image representations of the same class to be close to each other. Meanwhile, the representations of other classes are pulled away (see Fig. 6). However, this method requires a large batch size and thus the computational cost is high. It is also found that SupCon might result in class collapse, where all data samples of a class map to the same point in the latent space. Thus, an appropriate degree of spread of the representations of a certain class benefits the performance of models. Chen *et al.* [109] proposed a weighted class-conditional loss based on noise-contrastive estimation (InfoNCE [110]) to control the degree of spread. The loss helps better estimate the density of the distribution of positive samples. This improves the performance when the models are transferred to other tasks. As contrastive learning might be influenced by spurious correlation, where the learned representations do not completely catch meaningful semantics, a model based on empirical risk minimization (ERM) is used to predict spurious attributes, and its outputs are used to prepare positive and negative pairs in contrastive learning [111].

*Disentanglement learning.* Disentanglement learning is useful for enforcing invariance to specific characteristics or properties of images in the latent space by separating the content code, which represents the semantics of an image, and the style code, which represents appearance or other factors related to the operational scenarios. As common corruptions are forms of style, disentangled representations allow for models to use the content codes only for tasks like classification. This improves the corruption robustness since the content codes are invariant to different corruptions. As illustrated in Fig. 7, the style and content codes are learned by cross-domain transfer. A pair of autoencoders is used to transfer images from a domain containing brightness
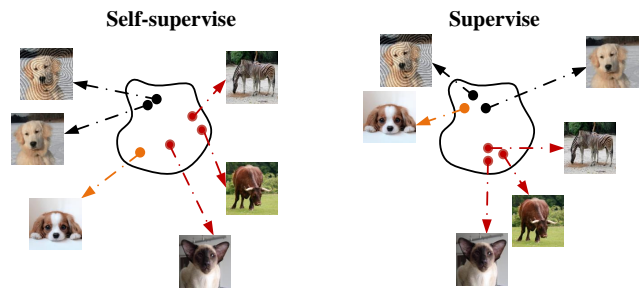


Fig. 6: Self-supervised and supervised contrastive learning [102]. Without ground truth labels, self-supervised learning may result in learning representations of images from the same class far away from each other in the latent space. For supervised learning, although the image representations of the same class are closer in the latent space, this might result in class collapse when images from the same class point to the same representation.
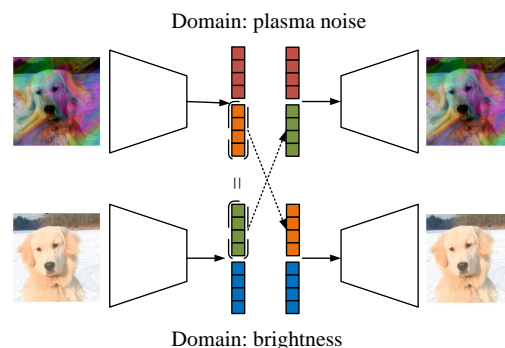


Fig. 7: Disentanglement learning, where the representation of images is separated into two parts— style code and content code. The content code represents the semantics of an image while the style code can represent the information of the type of corruption.

corruption to the other domain containing plasma noise. The content code extracted from the brightness domain together with the style code extracted from the plasma noise domain can be used to generate an image with plasma noise, and vice versa [103]. Being able to extract the content from different styles, models can be robust to different corruptions.

## 4.3 Knowledge distillation

The idea of knowledge distillation helps the models identify misguided information or filter out the correct information, thus contributing to increased generalization and corruption robustness. The framework of knowledge distillation needs at least two models: one as a teacher, and the other as a student, to distill information from one to another. To improve corruption robustness, the student model is set to distill invariant information w.r.t. image corruption from the teacher model. For instance, the auxiliary classifier in [37] assists the target model to learn invariant image representations regarding image corruptions. The target classifier

Fig. 8: General scheme of knowledge distillation. A student model can distill information from the teacher model, which can be pseudo labels [69], model weights [37], model predictions [37] or simulated domain/style information [39].

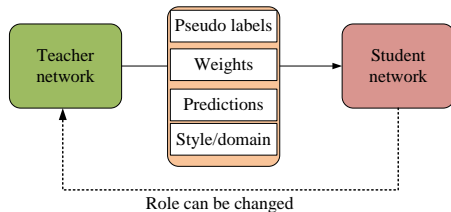is trained on original training images while the auxiliary classifier is trained on their augmented versions. Both classifiers share the same backbone, and the auxiliary classifier is trained to predict the same as the target classifier. Thus, the image representations of the original images and their augmented versions are close to each other in the latent space, ignoring the impact of image corruption. Instead of supervised learning, NoisyStudent [69] trains models by semi-supervised learning. It requires large amounts of data and computational resources. The teacher model is trained on labeled data to provide pseudo labels for the student model. The student model is trained on a larger unlabelled dataset along with the pseudo labels provided by the teacher model. The roles of the teacher and student models change iteratively. For the next iteration, the student model becomes the teacher model, while the teacher becomes the student. It shows robustness to image corruption as well as label noise. We provide a general scheme of knowledge distillation in Fig. 8. The student network can learn to distill information like pseudo labels, weights, predictions, and domain information from the teacher network. Moreover, the role of teacher and student can be changed during training.

## 4.4 Robust network layers

Robust network layers are designed to reduce the impact of data distribution shifts by modifying the receptive field of filters in certain layers in neural networks [35, 112] or normalizing the responses of intermediate layers [113, 114, 115]. Thus, they are intrinsically robust to common corruptions.

*Receptive field.* Receptive field modification involves changing or extending the kernels of a layer, which is often inspired by biological observations. A network with center blind-spot receptive fields is proposed in [35]. The noise in images is assumed to be pixel-wise independent, and thus the receptive field obtained from the pixels around can help reduce the influence of noise. Further, Laine *et al.* combine the receptive fields of a blind-spot network in four directions [112]. The network is robust to noise but not other corruptions. Motivated by the biological behavior of neurons in the human visual system, a push-pull layer is proposed in [116] and deployed as a substitute of convolutional layers [117]. It is based on a response inhibition that suppresses the response to noise and spurious texture. Similarly, the on-/off-kernels [118] are two Gaussian kernels following opposite directions and encourage excitatory center or inhibitory surround, which is shown to be beneficial to

robustness under different illumination conditions. Spatial smoothing kernel [119] provides stabilized feature maps that might smooth the loss landscape. This work further explains the improved generalization of DNNs using global average pooling, ReLU6, and other similar techniques, as they have a similar effect on smoothing the responses of models. Recent works on sparse neural networks (SNNs) find that a compact model benefits corruption robustness, compared with its dense version [120, 121]. Instead of training an entire SNN, Locally Competitive Algorithm (LCANet) [122] uses sparse coding layers in the front end via lateral competition, which is inspired by a biological observation that neurons inhibit their neighboring neurons which have similar receptive fields.

*Normalization.* Normalization layers are originally designed to speed up the training process, by normalizing the distribution of the inputs of intermediate layers [113, 115, 114]. Subsequently, researchers showed that the Batch Normalization (BN) layer also improves the robustness of DNNs towards adversarial attacks [123], image corruptions [124], domain shift [125, 126], by simply rectifying the statistics of BN layer according to the new test data (Adaptive-BN). However, BN requires a batch of images to calculate the representative mean and variance. A single image is not enough to obtain representative statistics for the test data, limiting the deployment of Adaptive-BN in real applications. Instance normalization (IN) is originally designed to achieve better style transfer, where the feature maps are normalized using the mean and variance of each channel of each sample [115]. It was demonstrated in [127] that IN is robust to specific types of corruption (haze, fog, and smoke). Instead of normalizing in the spatial domain, convolutional normalization [128] performs normalization in the frequency domain of kernels of convolutional layers, which is shown to be robust to adversarial attacks and label noise.

## 5 PERFORMANCE COMPARISON

To ensure fair and unbiased comparison of model robustness performance, we build a unified evaluation framework that includes all relevant metrics and benchmarks. Currently, there is a lack of such a framework to evaluate corruption robustness. As a result, the most commonly used benchmark—ImageNet-C may not be representative of the overall corruption robustness of a model. We noticed that the results collected from the literature were computed using different baselines when calculating the mCE and mFP. This makes it unfair to compare different works directly. In our framework, we use a standardized set of benchmarks when evaluating model robustness, including ImageNet-C, ImageNet-C̄, ImageNet-P, and ImageNet-3DCC. Moreover, when computing evaluation metrics like mCE and mFP, we use the same baseline. By doing so, we can ensure that the results are comparable and that the evaluation is fair and unified. We thus release a benchmark suite and evaluate the corruption robustness of well-known ImageNet pre-trained models and a few state-of-the-art techniques addressing corruption robustness.

TABLE 2: Overview of methods addressing corruption robustness, organized in four categories and with brief descriptions of their characteristics.

| Category | Method | Codes | Remark |
|---|---|---|---|
| **Data Augmentation** | AutoAugment [80] | Yes | Apply reinforcement learning to learn the best augmentations |
| | AugMix [38] | Yes | Combine different augmentations randomly and use Jensen-Shannon Divergence to ensure the consistency between source and augmented images |
| | AugMax [82] | Yes | Adversarially select augmentations and their combined weights |
| | AugSVF [81] | No | Expands the options of operations in AugMix |
| | Mixup [75] | Yes | Linearly interpolate input examples and their ground truth |
| | Gaussian Patch [74] | Yes | Small patches of Gaussian noise are added randomly |
| | RobustMix [76] | No | Frequency bands of input samples are mixed, and their weights depend on the relative amount of energy |
| | Targeted Aug [85] | No | Copy-paste the predictive features of images that may vary across different domains |
| | Adversarial Aug [96] | No | Use adversarial noise in training |
| | Test-time Aug [84] | Yes | Augmentations to use are selected based on the characteristics of test data |
| | PRIME [83] | Yes | Augmentations with maximum entropy are selected during training |
| | Adv. Noise Propagation [98] | | Adversarial noise is injected into hidden layers |
| | NoisyMix [99] | No | Apply adversarial noise in both input and feature space |
| | DAJAT [100] | Yes | Combine common augmentation together with adversarial training, improving the efficiency of the used augmentations |
| | ME-AdA [129] | Yes | A maximum-entropy-based regularization term is used in adversarial training, which perturbs the distribution of data instead of the data itself |
| | LISA (Selective Aug) [79] | Yes | samples with the same label but in different domains or samples in the same domain but with different labels |
| | $L_p$–AT [52] | Yes | $L_p$ Adversarial Training |
| | GAT [93] | No | Gaussian noise generate adversarial examples |
| **Representation Learning** | G-SimCLR [108] | Yes | Contrastive learning with pseudo labels trying to avoid representation of the same category to be distant |
| | SupCon [102] | Yes | Contrastive learning with ground truth labels to ensure the positive and negative samples are from different categories within one batch |
| | Balanced-SupCon [109] | Yes | Apply InforNCE loss to avoid class collapse |
| | Self-learning [59, 104] | No | self-supervised learning for robust representations |
| | Perceptually-similar representation learning [106] | No | Representations of perceptually similar images are learned to be similar |
| | Adv. Con [107] | Yes | Contrastive learning with adversarial noise |
| | SimCLR [105] | Yes | Self-supervised contrastive learning |
| | CNC [111] | Yes | Contrastive learning helps mitigating learning spurious correlations |
| **knowledge distillation** | NoisyStudent [69] | Yes | A teacher network trained on cleaned data distills information to a student network, and the roles of teacher and student change iteratively |
| | Auxiliary training [37] | Yes | Force an auxiliary classifier to predict corrupted data correctly, implicitly learning invariant representation in terms of corruptions |
| **Robust Network Layer** | AdaBN [124] | No | Adapt BN statistics to fit new dataset |
| | Push-pull Layer [116] | Yes | Biologically-inspired kernels result in robust response |
| | On-off Center-surround Kernels [118] | Yes | Gaussian kernels with opposite directions |
| | Spatial Smoothing Kernel [119] | Yes | Kernel results in stabilized feature maps |
| | Winning hand [120] | No | Compressed networks from over-parameterized models |
| | LCANet [122] | Yes | Apply sparse coding layers in the front end |

TABLE 3: Results of ImageNet pre-trained backbone networks on ImageNet corruption benchmark datasets. The top-3 mCE on each benchmark dataset are highlighted. Baseline: ResNet18.

| Architecture | Networks | #Params (M) | ImageNet | | | | |
|---|---|---|---|---|---|---|---|
| | | | C | C̄ | 3DCC | P | |
| | | | mCE (%) | mCE (%) | mCE (%) | mFP (%) | mT5D (%) |
| CNN | ResNet50 [130] | 97.5 | 91.17 | 92.63 | 91.5 | 65.64 | 109.39 |
| | ResNet101 [130] | 169.9 | 87.64 | 88.5 | 88.47 | 52.37 | 77.19 |
| | WideResNet50-2 [131] | 262.8 | 88.58 | 87.45 | 89.45 | 51.83 | 84.66 |
| | ResNeXt50d (32×4d) [132] | 95.5 | 92.45 | 94.21 | 93.08 | 65.69 | 91.91 |
| | ResNeXt101 (64×4d) [132] | 318.3 | 86.45 | 86.93 | 88.07 | 46.29 | 66.83 |
| | DenseNet121 [133] | 30.4 | 93.96 | 95.67 | 94.33 | 76.86 | 92.91 |
| | EfficientNet-B2 [134] | 34.8 | 91.62 | 91.82 | 92.54 | 54.61 | 72.63 |
| | CoatNet-nano [135] | 57.8 | 89.52 | 89.43 | 92.06 | 63.6 | 87.06 |
| | ConvNext-B [136] | 338.0 | 84.43 | 84.2 | 86.59 | 34.01 | 74.8 |
| | ConvNext-L [136] | 754.4 | 83.74 | 83.26 | 85.68 | 30.20 | 74.94 |
| Transformer | BiT-ResNet-v2 (50×1) [137] | 97.5 | 86.3 | 85.62 | 88.43 | 45.74 | 68.80 |
| | Swin-B [138] | 334.8 | 83.47 | 81.46 | 85.83 | 41.36 | 84.06 |
| | Swin-L [138] | 749.7 | **81.84** | **80.05** | 84.15 | 33.14 | 75.63 |
| | VOLO-D3 [139] | 329.3 | 83.65 | 84.72 | 85.12 | 29.84 | 55.55 |
| | VOLO-D5 [139] | 1127.074 | 82.44 | 83.68 | **84.24** | **26.44** | **54.95** |
| | Vit-B/8 [140] | 330.2 | 88.19 | 86.77 | 92.13 | 81.59 | 85.48 |
| | BEiTv2-B [141] | 330.1 | **80.87** | **79.75** | **83.72** | **28.36** | **54.43** |
| | BEiTv2-L [141] | 1161.3 | **77.74** | **77.06** | **80.69** | **19.93** | **43.68** |
| | EdgeNeXt-B [142] | 70.6 | 86.17 | 87.02 | 87.76 | 32.17 | 57.47 |
| | MViTv2-B [143] | 196.3 | 83.34 | 81.82 | 85.71 | 36.52 | 81.25 |
| | MaxVit-S [144] | 247.6 | 85.3 | 83.52 | 87.34 | 38.52 | 128.6 |

## 5.1 Pre-trained ImageNet backbones

Evaluating model robustness to common corruptions is not usually performed when benchmarking new computer vision backbones. We conducted a thorough investigation of the performance and robustness of existing backbone models. We designed a unified benchmark suite that includes metrics for evaluating corruption robustness on several available datasets, such as ImageNet-C, ImageNet-C̄, ImageNet-3DCC, and ImageNet-P[1]. We used ImageNet pre-trained ResNet18 as the baseline model and report the results in Table 3. Our findings demonstrate the robustness of commonly used computer vision models in the face of corrupted images.

Transformers have shown great potential in improving corruption robustness, as evidenced by the fact that the top three backbones on all four benchmarks are based on transformers. However, their large model size can limit their applications, as they require significantly more computational resources and are pre-trained on large datasets. In Fig. 9, we analyze the relationship between the number of parameters and the mCE achieved by 21 backbones[2] in the ImageNet-C, ImageNet-C̄, and ImageNet-3DCC benchmarks. We observe that, except for the models having more than 500 million parameters, the number of parameters and the mCE follow a linear relation (as shown by the blue lines in Fig. 9). Increasing the model size beyond a certain threshold does not necessarily guarantee a corresponding improvement in corruption robustness, as the improvement might eventually reach a point of saturation beyond which additional model size does not yield further benefits. Other techniques that focus on data itself, such as methods that efficiently exploit available, limited data during training, need further investigation.

## 5.2 Methods addressing corruption robustness

We collect the robustness results of existing approaches on CIFAR-C and ImageNet-C benchmark datasets and report them in Table 4 and Table 5.

Most methods with benchmark results on CIFAR–C and ImageNet-C rely heavily on data augmentation techniques, while many methods from the other three categories do not follow a standard evaluation process to measure corruption robustness. For instance, they only use subsets of the available benchmarks. This highlights the need to establish a standardized evaluation procedure to ensure that models are tested consistently, allowing for a fair comparison of performance. Most of the robustness analyses of ImageNet-trained models are done solely on ImageNet-C, while other benchmark datasets such as ImageNet-C̄ and ImageNet-3DCC were largely ignored. We suggest incorporating other available corruption benchmarks to provide a more complete and comprehensive performance evaluation.

Furthermore, different works chose different baselines for comparison when using corruption robustness metrics like mCE. In some cases, only the error rate of the models on the corruption benchmarks was used for evaluation. As a result, the obtained values of mCE or other corruption robustness metrics are non-unified and non-directly compa-

---

1. Codes will be made available in the near future for the benefit of the research community.

2. We will release the results of more backbones when they become available.
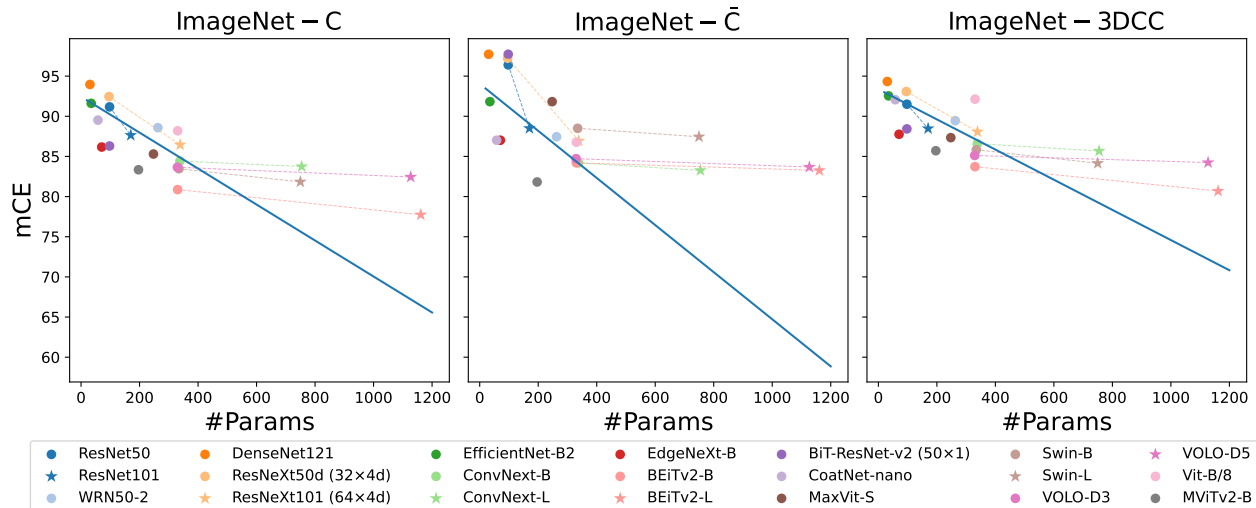
Fig. 9: The size of backbones versus $\mathrm{mCE}$ on ImageNet-C, ImageNet-$\bar{\mathrm{C}}$, and ImageNet-3DCC. The mCE does not decrease linearly with an increase in model size. This demonstrates that a larger model is not an effective solution to improving corruption robustness, as the additional computational cost does not provide the expected benefits.

rable[3].

We report the error rate of models on CIFAR in Table 4 and compare the model performance based on it, as $\mathrm{mCE}$ are not directly comparable when using different baselines. We found that CARD+LRR+WideResNet-18 [120] (from the category: robust network layer) achieved the best error rate on both datasets. This approach involves complex algorithms for learning a sparse neural network, which results in a compressed model size but increases the training time significantly. AugMax+ResNeXt29 [82], which augments images with adversarially selected augmentations, achieved the second-best error rate.

Among the augmentation-based approaches, Aug-Max [82] performed the best on both the original test set of CIFAR and its corrupted versions, with the lowest error rate. AugMax selects augmentations randomly and combines them with weights computed adversarially, leading to the worst-case of mixtures. This is why it performs better than AugMix and AutoAugment, where augmentations and combination weights are sampled randomly or learned, respectively. Although using adversarial noise during training can improve the corruption robustness [52, 93], augmentations using spatial transformation lead to more outstanding improvements, as demonstrated by e.g. AugMix [38] and AugMax [82].

In Table 5, we report the results on ImageNet. NoisyStudent+EfficientNet-L2 [69] performs the best on ImageNet-C. Models with the second and third-best error rates are AdaBN+ResNeXt101 and AdaBN+DenseNet161 [124]. NoisyMix+ResNet50 [99] has the fourth-best robust error rate. NoisyStudent [69] uses a dual-network architecture to extract useful information from millions of unlabelled images, which demands significant computational resources. The model was trained using augmentations that partially overlapped with those in ImageNet-C.

As a result, it would be unfair to compare it directly with other models on this benchmark dataset.

Adaptive batch normalization layer [124] rectifies BN statistics that better fit the test data. The two models with the second and third-best error rates have a marginally large model size compared to those used by the augmentation-based methods. However, a major benefit of this method is its low computational requirements to rectify the statistics.

NoisyMix [99] performs data augmentation in both input and feature space. Thus, the complexity of the augmented training data is higher than those augmented by AugMax, thus gaining more improvement. This demonstrates that augmentation in feature space benefits corruption robustness and is worth more investigation.

These approaches commonly benefit from either large-scale training datasets or high-capacity models. However, as shown in Fig. 9, increasing model size alone does not guarantee a corresponding improvement in corruption robustness. Therefore, future research should focus on developing effective learning methods with limited data and computational resources.

## 6 INDIRECT APPROACHES

In this section, we review techniques that may improve corruption robustness, despite their evaluation process does not explicitly account for such robustness. We refer to them as indirect methods in this survey. Although these methods are not specifically designed to improve corruption robustness, they may provide valuable insights that are worth further investigation. Our focus is not on benchmarking these methods, but rather on providing a broader perspective on potential ways to improve corruption robustness. For instance, image restoration can improve image quality by removing the effect of corruptions, and thus models can have better performance on well-restored images. Regularization avoids overfitting, and robust optimization aims at optimizing the objective function under the worst-case. Both

---

3. The results of existing methods tested on our benchmark framework will be provided in the future.

TABLE 4: Results on CIFAR-10/100 and CIFAR-10/100-C. The **err** stands for the error rate on the original test set, **robust err** indicates the error rate on the corrupted versions and **mCE** is the mean corruption error.

| Category | Method | CIFAR-10 | | | CIFAR-100 | | | baseline |
|---|---|---|---|---|---|---|---|---|
| | | err | robust err | mCE (%) | err | robust err | mCE (%) | |
| Data augmentation | AugMix+AllConvNet [38] | — | 15 | — | — | 42.7 | — | — |
| | AugMix+DenseNet [38] | — | 12.7 | — | — | 39.6 | — | — |
| | AugMix+WideResNet [38] | — | 11.2 | — | — | 35.9 | — | — |
| | AugMix+ResNeXt [38] | — | 10.9 | — | — | 34.9 | — | — |
| | AutoAugment+AllConvNet [38] | — | 29.2 | — | — | 55.1 | — | — |
| | AutoAugment+DenseNet [38] | — | 26.6 | — | — | 53.9 | — | — |
| | AutoAugment+WideResNet [38] | — | 23.9 | — | — | 49.6 | — | — |
| | AutoAugment+ResNeXt [38] | — | 24.2 | — | — | 51.3 | — | — |
| | Adv. Training+AllConvNet [38] | — | 28.1 | — | — | 56 | — | — |
| | Adv. Training+DenseNet [38] | — | 27.6 | — | — | 55.2 | — | — |
| | Adv. Training+WideResNet [38] | — | 26.2 | — | — | 55.1 | — | — |
| | Adv. Training+ResNeXt [38] | — | 27 | — | — | 54.4 | — | — |
| | Mixup+AllConvNet [38] | — | 24.6 | — | — | 53.4 | — | — |
| | Mixup+DenseNet [38] | — | 24.6 | — | — | 55.4 | — | — |
| | Mixup+WideResNet [38] | — | 22.3 | — | — | 50.4 | — | — |
| | Mixup+ResNeXt [38] | — | 22.6 | — | — | 51.4 | — | — |
| | AugSVF+WideResNet [81] | 5.2 | 9.9 | — | 24.9 | 34.8 | — | — |
| | AugMax+ResNet18 [82] | 4.24 | 9.64 | — | 21.31 | 34.25 | — | — |
| | AugMax+WRN40-2 [82] | 4.32 | 9.33 | — | 23.2 | 33.65 | — | — |
| | AugMax+ResNeXt29 [82] | **3.61** | **7.89** | — | **19.3** | **31.14** | — | — |
| | AdA+EDSR [96] | — | — | 15.47 | — | — | — | *Not disclose* |
| | AdA+EDSR+AugMix [96] | — | — | 9.4 | — | — | — | *Not disclose* |
| | AdA+EDSR+AugMix+DeepAugment [96] | — | — | 7.83 | — | — | — | *Not disclose* |
| | ME-ADA+AllConvNet [129] | — | 21.8 | — | — | 48.8 | — | — |
| | ME-ADA+DenseNet [129] | — | 23.1 | — | — | 52.2 | — | — |
| | ME-ADA+WideResNet [129] | — | 16.7 | — | — | 47.2 | — | — |
| | ME-ADA+ResNeXt [129] | — | 16.6 | — | — | 42.7 | — | — |
| | ANP+VGG16 [98] | — | **8.3** | 75.7 | — | — | — | VGG16 |
| | Gaussian patch+ResNet18 [37] | 4.87 | — | 63.17 | — | — | — | AlexNet |
| | Gaussian patch+WRN50 [37] | 4.34 | — | 66.63 | — | — | — | AlexNet |
| | Gaussian patch+ResNeXt50 [37] | 4.48 | — | 66.63 | — | — | — | AlexNet |
| | GAT+WRN-40-2 [93] | 5.9 | 14.6 | — | 25.6 | 40.7 | — | — |
| | GAT+AugMix+WRN-40-2 [93] | 4.7 | 9.9 | — | 24.5 | 34.6 | — | — |
| | Test-time-Aug-k-2-Flip + Wide-ResNet [84] | — | — | — | — | 32.6 | — | — |
| | PRIME+ResNet18 [83] | 5.8 | 10.2 | 10.2 | **21.6** | **31.8** | 31.8 | *Not disclose* |
| | DAJAT-Base-2*AA + WRN-34-10 [100] | 11.29 | 19.88 | — | 31.25 | 43.05 | — | — |
| | $L_\infty$–AT + ResNet18 [52] | 6.7 | 17.3 | — | — | — | — | — |
| | $L_2$–AT + ResNet18 [52] | 6.4 | 16.6 | — | — | — | — | — |
| Representation learning | Self-sup (rotation)+WRN-40-2 [104] | — | 23.1 | — | — | — | — | — |
| | ACL(DS)+ResNet18 [107] | 17.81 | 47.18 | — | — | — | — | — |
| knowledge distillation | Auxiliary training + ResNet18 [37] | 3.98 | — | 57.01 | 20.53 | — | 69.34 | AlexNet |
| | Auxiliary training + Wide-ResNet50 [37] | 3.51 | — | 55.41 | 19.16 | — | 68.89 | AlexNet |
| | Auxiliary training + ResNeXt50 [37] | 3.66 | — | 49.37 | 18.49 | — | 69.13 | AlexNet |
| Robust network layer | AdaBN+ResNet20 [124] | — | 27 | 90.7 | — | 55.5 | 87.4 | AlexNet |
| | AdaBN+ResNet56 [124] | — | 18.6 | 63 | — | 52 | 81.9 | AlexNet |
| | AdaBN+ResNet18 [124] | — | 15.7 | 53 | — | — | — | AlexNet |
| | AdaBN+ResNet50 [124] | — | 16.9 | 57.6 | — | — | — | AlexNet |
| | AdaBN+VGG19 [124] | — | 19 | 63.7 | — | 48.6 | 76.6 | AlexNet |
| | AdaBN+WRN28-10 [124] | — | 13.2 | 44.5 | — | 34.7 | 54.8 | AlexNet |
| | AdaBN+ResNeXt29 [124] | — | 14.5 | 49.9 | — | 34 | 53.7 | AlexNet |
| | AdaBN+DenseNet [124] | — | 12.4 | 42.4 | — | 34.2 | 54.2 | AlexNet |
| | Push-pull+ResNet56 [116] | — | 26.33 | 91 | — | — | — | AlexNet |
| | Push-pull+DenseNet100-24 [116] | — | 21.37 | 73 | — | — | — | AlexNet |
| | CARD+LRR+WideResNet-18 [120] | **3.2** | **7.25** | — | **19.4** | **28.7** | — | AlexNet |

TABLE 5: Results on ImageNet and ImageNet-C.The **err** stands for the error rate on the original test set, **robust err** indicates the error rate on the corrupted versions and mCE is the mean corruption error.

| Category | Method | ImageNet | | | |
| | | err | robust err | mCE (%) | baseline |
|---|---|---|---|---|---|
| Data augmentation | AugMix+SIN+ResNet50 [38] | 25.2 | — | 64.9 | AlexNet |
| | AugMix+ResNet50 [38] | 22.4 | — | 68.4 | AlexNet |
| | SIN+ResNet50 [38] | 27.2 | — | 73.3 | AlexNet |
| | Random AutoAugment+ResNet50 [38] | 23.6 | — | 76.1 | AlexNet |
| | AutoAugment+ResNet50 [38] | 22.8 | — | 72.7 | AlexNet |
| | AugMax+DuBIN+ResNet18 [82] | 32.38 | 64.99 | 82.56 | AlexNet |
| | DeepAugment+AugMax+ResNet18 [82] | 35.57 | 53.45 | 68.47 | AlexNet |
| | Test-Aug-k-2-H-Flip+AugMix+ResNet50 [84] | 22.37 | 64.55 | — | — |
| | PRIME+ResNet50 [83] | 23 | 55 | 57.5 | *Not disclose* |
| | PRIME+DeepAugment+ResNet50 [83] | 24.5 | 59.9 | 51.3 | *Not disclose* |
| | RobustMix+ResNet50 [76] | 22.9 | — | 61.2 | AlexNet |
| | RobustMix+EfficientNet-B0 [76] | 23.2 | — | 61.9 | AlexNet |
| | AdA+All [96] | 26.8 | — | 75.03 | AlexNet |
| | AdA+Augmix+All [96] | 28.32 | — | 72.2 7 | AlexNet |
| | AdA+DeepAugment+All [96] | 29.39 | — | 65.54 | AlexNet |
| | NoisyMix+ResNet50 [99] | **22.4** | **47.7** | — | — |
| Representation learning | SupCon+ResNet50 [102] | 21.3 | — | 67.2 | AlexNet |
| | SupCon+ResNet200 [102] | — | — | 50.6 | AlexNet |
| knowledge distillation | Auxiliary training+ResNet18 [37] | 30.06 | — | 78.86 | AlexNet |
| | Auxiliary training+ResNet34 [37] | 25.86 | — | 75.58 | AlexNet |
| | NoisyStudent+EfficientNet-L2 [69] | **11.6** | **22.2** | 28.3 | AlexNet |
| Network layer | AdaBN+ResNet18 [124] | — | 58.2 | — | — |
| | AdaBN+ResNet50 [124] | — | 51.3 | — | — |
| | AdaBN+VGG19 [124] | — | 54.5 | — | — |
| | AdaBN+WRN101 [124] | — | 48.3 | — | — |
| | AdaBN+ResNeXt101 [124] | — | **46.1** | — | — |
| | AdaBN+DenseNet161 [124] | — | **45.3** | — | — |

can improve the generalization performance of models, potentially improving corruption robustness. Shortcut learning mitigation encourages models to learn more task-related semantics, instead of the shortcut solutions in data. This might also benefit corruption robustness, as models learn to focus on meaningful semantics that is invariant to corruptions. Moreover, understanding the learning behavior of models might provide useful insights for designing methods addressing corruption robustness.

## 6.1 Image restoration

The first extensive and systematic benchmark of corruption robustness in image classification was proposed in 2019 [32], and earlier studies focused mostly on image restoration, e.g. image denoising [34]. To remove noise in an image, the basic approach is to smooth it with an average medium or Gaussian filter. However, the filtering causes the loss of high-frequency information which might be essential for recognition tasks [71]. An autoencoder can be trained to remove different corruptions with one network [34, 112]. To reconstruct images without corruption, pairs of corrupted and clean images are needed. The corrupted images are usually generated synthetically from the clean images, with fixed levels of noise. This causes the trained autoencoders to have limited adaptability to other noise levels and types than those used for training. To improve this, a feedback mechanism is used to generate images with different levels of noise during training [33]. This mechanism adjusts dynamically the noise level in the images, and thus the autoencoder is generalized to different levels of noise. The inconvenience of training denoising autoencoders is the prerequisite for clean and corrupted image pairs. An algorithm [34] for training

an autoencoder with corrupted images only was shown to be capable of removing photographic noise. However, it is based on a strong assumption that the noise is zero-mean, which may limit its applicability to a wider scope of cases. Based on the zero-mean assumption, a non-local filtering layer [145] can extract the non-local self-similarity features of images, which generalize to different noise levels.

With a more complex training framework, Mimic-GAN [39] was designed to simulate corruptions in images by an auxiliary model and reconstruct the images without corruptions. The simulated corruptions are compared with true corruptions. With the latent representations including the corruption information, the latent representations without corruptions can be found in the manifold of a pre-trained GAN. However, the quality of the generated images is greatly limited by the performance of the GAN, and thus more exploration is needed to improve the image quality.

## 6.2 Regularization

Regularization can avoid overfitting and improve the generalization of DNNs. Thus, when there are unseen corruptions during testing, models trained with proper regularization techniques may show better corruption robustness. The regularization techniques can be applied to three aspects: activation functions, weights of neural networks, and output distributions.

The activation regularization penalizes large activations and encourages small activations. It can encourage the networks to learn sparse representations with $L_1$ regularizer applied to the activations of layers [146]. For weight regularization, techniques like weight decay ($L_1$ or $L_2$ penalty) [147], dropout [148], and weight uncertainty [149]

are used. Weight decay applies the $L_1$ or $L_2$ norm of weights as a penalty term in the objective function. It forces the networks to learn small weight values, reducing overfitting [147]. Despite adding a penalty term to objective functions, dropout [148] throws away some nodes of a NN randomly, making the model sparse and avoiding overfitting. Instead of regularizing the weight values, Bayesian Neural Networks (BNNs) [149] bring uncertainty to the weights of neural networks by training an ensemble of models. The models learn the distributions of the weights. When the model is tested, its weights are sampled from the learned distribution. This improves the generalization of the DNNs on unknown data. For output regularization, Pereyra *et al.* [150] proposed a regularizer based on the entropy of the predictions of DNNs. A low entropy prediction indicates a reliable prediction. This can smooth the output distributions and eliminate sharp distributions. Wang *et al.* [151] focused on the outputs of intermediate layers and regularized their predictive power to avoid large impacts of local features on the predictions, by an extra classifier. It predicts the learned representations of the earlier layer at each location, resulting in a prediction map recording the prediction results. Thus, the map has the same size as the response of the earlier layer. Contrasting with the regular classifier in the network, the extra classifier is trained to predict wrongly. Therefore, the regular classifier pays more attention to global features, as the other classifier using local features has a negative impact on the predictions. The authors in [152] regularized the outputs of each layer in neural networks. For samples in the same categories, the model learns fewer peaky representations, resulting in smoother class boundaries and thus improving the generalization of models.

### 6.3   Robust optimization

Robust optimization (RO) aims at improving the robustness of decision-making models to uncertainty that might be caused by unexpected inputs [153]. Among the RO techniques, distributionally robust optimization (DRO) minimizes the worst-case error to improve the model robustness to unknown OOD data [154, 155, 156]. In DRO, data collected from different environments is a prerequisite. Therefore, the worst-case error corresponds to the highest error of the model performing in one of the environments. The objective of the optimization is:

$$arg \min_{f} \sup_{Q \in P(P_{tr})} E_{X,Y \sim Q}[l(f(X), Y)], \qquad (12)$$

where $f$ is the model, $X$ is the data, $Y$ is the ground truth label, $l$ is the loss function, and $P(P_{tr})$ indicates the training sets with different data distributions. Due to the complexity of a convex optimization problem, the authors in [157] approximate the worst-case expected value through Bayesian optimization. Rather than optimizing the performance of a model in terms of the worst-case, invariance-based optimization (IBO) aims at finding the invariant information towards distribution shifts, with data collected from multiple environments [158, 159].

RO-based methods can improve the generalization of models to future uncertainty, and it would be beneficial to investigate their contribution to the corruption robustness of the models.

### 6.4   Shortcut learning mitigation

Bias in data can affect how models use the data to achieve their tasks [160]. One example is shortcut learning. Shortcuts are simple solutions in data and harm the OOD generalization performance of models. They result from spurious correlations between data and ground truth labels that ignore task-related semantics [24]. For instance, the embedded text in the images of class 'horse' induces the models to predict images with the text as a horse, even if the images do not contain horses (see Fig. 1a) [30]. The models do not generalize well to other images with horses but without the text. In another case, a model simply using a unique background color as a defining feature to predict a certain object lacks robustness to certain types of corruption that change the background of images.

Forcing models to learn more meaningful task-related semantics, shortcut learning mitigation is promising to improve generalization as well as corruption robustness. The authors in [161] first identify shortcuts in a medical image dataset, which are colored patches in images of benign cases. Then, they embedded similar colored patches in images of malignant cases. The networks learn to ignore the spurious correlations to the colored patches. Moreover, there might be visually unobservable shortcuts implicitly existing in data, e.g. frequency shortcut [162] which is a specific small set of frequencies that corresponds to textures or shapes in the spatial domain and can be used to achieve classification for a certain class easily. However, the frequency-removal-based algorithm [162] can only provide a rough estimation of the learned frequency shortcuts. Thus, the explicit identification of imperceptible shortcuts is still challenging.

Without identifying the shortcuts, it could be difficult to mitigate their influence. To solve this, a regularization term [163] decoupling feature learning dynamics makes the identification of shortcuts unnecessary. During training, NNs learn from as many features as possible instead of a subset of features which minimizes cross-entropy loss. In [164], samples with a high shortcut degree distill less information to DNNs during training. The shortcut degree is measured by comparing the integrated gradients of prediction in terms of input at the early training stage and after training, because samples with shortcut features are preferred early in the training process. The approach is designed for Natural Language Understanding (NLU) models, but it can be also adapted to computer vision. For instance, instead of using the integrated gradient of predictions to evaluate shortcut degree, an auxiliary network with low capacity is used to identify the amount of shortcut information contained in images [165]. With the measured shortcut degree per training sample, the target network with high capacity can learn less from images with high shortcut degrees. The approach was shown to be feasible to synthetic shortcuts (e.g. a horizontal line and Gaussian noise). Further investigation is needed for its feasibility to implicit shortcuts in the data.

Dataset bias, as one of the reasons for shortcut learning, urges researchers to develop approaches targeting its mitigation. The work in [166] uses gradient-based scores to detect minority samples that induce bias, preventing the models from learning shortcut features caused by data bias.

Minderer *et al.* [167] proposed automatic shortcut removal in self-supervised representation learning. They utilized adversarial training to avoid NNs learning shortcut features like watermarks (e.g. when images of only one class have watermarks — a simple and common feature, NNs tend to use the feature for the classification of the class). The difference between adversarial perturbed images and the source images helps inspect the possibly learned shortcuts. The authors in [168] examined shortcut features in contrastive learning. They observe that the difficulty in distinguishing positive and negative images affects the predictability of extracted features. Implicit Feature Modification (IFM) [168] adds adversarial perturbations to the representations and allows models to learn from more predictive features without suppressing other good features. It outperforms state-of-the-art contrastive learning such as SimCLR [101] and Mocov2 [169]. But for simple tasks like color classification, the extracted features are complex and thus redundant. The definition of shortcut features needs more consideration instead of being limited to the complexity of extracted features.

The methods addressing shortcut learning mitigation facilitate a deeper understanding of the learning behavior of the models. Although they are not designed to improve corruption robustness, they may provide a good inspiration for future work on robustness. For instance, we can design approaches to avoid unwanted learning behaviors that impair robustness.

## 7 CHALLENGES AND FUTURE OPPORTUNITIES

Corruption robustness is crucial for the deployment of computer vision models in safety-critical applications, e.g. autonomous-driving [4]. While there have been significant advances, several challenges, and opportunities remain for improving the corruption robustness of these models. We discuss here some of these challenges and suggest possible directions for future research.

*Coverage of potential corruption types and levels in the real world.* One of the primary challenges in improving corruption robustness is extensively addressing corruption types and levels in real-world scenarios. The corruptions encountered in the real world can be more diverse than those included in the benchmark datasets, and a model may fail to generalize well to all these corruptions unseen during training. With limited data and computational resources, developing methods that can learn to handle a wide range of corruptions becomes critical. One way to address this challenge is to collect and annotate large-scale datasets that include diverse types of corruption. However, this is a time-consuming and expensive process. Augmentation-based approaches are currently the best solution, while the generation of synthetic corruptions needs further investigation to ensure the generated corruptions are sufficiently representative of real-world corruptions. This further supports future research on developing methods that can effectively transfer knowledge from synthetic to real-world corruptions.

*Investigation of architectures and training frameworks.* While data augmentation is an effective method for improving corruption robustness, the other three categories of methods (representation learning, knowledge distillation, and robust network layer) that focus on structural and architectural changes, need more investigation. Compared to augmentation-based methods which may overfit the robustness to corruptions seen during training, there are fewer methods and limited benchmark results for these approaches. Further investigation is required to improve the capability of these methods in learning robust representations that can be transferred to other tasks, distilling knowledge that is robust to corruptions, and being intrinsically robust to corruptions. These techniques are promising for improving model robustness and their potential benefits warrant further research to better understand their capabilities and limitations.

*Effective training strategies with less computational resources.* While large models and dataset size can benefit corruption robustness to some extent, the computational resources needed for training might not always be available. This could limit the reproducibility and usability of the methods. For instance, the backbone of NoisyStudent [69] has more than 1.8 billion parameters and was trained using a vast amount of unlabelled images. Therefore, it is essential to develop efficient training strategies that can achieve the same level of corruption robustness with limited data and computational resources. This can involve techniques such as transfer learning [170], meta-learning [171], and few-shot learning [172], leveraging prior knowledge to learn from limited data. Transfer learning distills knowledge from one dataset to another. Thus, a model pre-trained on a large-scale dataset can provide prior information that is useful for the transferred tasks. Meta-learning uses an outer algorithm to optimize e.g. the learning speed or the generalization performance of the inner algorithm, i.e. the target task. Few-shot learning aims at learning with few or zero samples by matching similar classes that are seen during training. With these methods, the limited data and computational resources can be used efficiently.

*Linking corruption robustness, OOD generalization, and shortcut learning mitigation.* Corruption robustness and OOD generalization are closely related as common corruptions are a cause of data distribution shifts from the distribution of the training data. Shortcut learning, where a model relies on spurious correlations in the data to achieve high accuracy, can also impact corruption robustness. We find it necessary to consider these three aspects when targeting the performance evaluation of models, and them to become part of standard practices in the performance evaluation process. The evaluation of robustness and generalization from multiple perspectives can yield more comprehensive and trustworthy results. Moreover, theoretical analysis that focuses on explaining the learning behavior of models [173, 174] and the factors guaranteeing OOD generalization [175, 54] might help to better understand the intrinsic reasons for the impaired corruption robustness of computer vision models, potentially guiding the design of approaches for improving robustness. Regarding shortcut learning, it is important to develop methods that can identify and mitigate shortcut learning to provide a clearer understanding and evaluation of the generalization properties of models, and to enforce the learning of more task-related semantics.

Improving the corruption robustness of computer vision models is a challenging task, and requires the development

of effective techniques that can handle diverse corruptions. In some cases, applications have hardware constraints on the site of training. Thus, designing robust methods that can operate with limited training data and computational resources is a promising direction to explore. Large-capacity models are not the best solution to guarantee corruption robustness, though they might achieve brilliant performance on benchmarks. Smaller models can also be robust if they can distill proper knowledge from other models. Inducing bias [176] in the form of priors or expert knowledge is thus another promising direction. Future research should focus on investigating methods of all four categories, improving the connection among corruption robustness, OOD generalization, and shortcut learning mitigation. Achieving these goals will foster progress toward the safe and reliable deployment of computer vision models in real-world applications.

## 8 CONCLUSIONS

Corruption robustness is one crucial aspect of the performance evaluation of computer vision systems, as it indicates how well a model can operate in the presence of image corruption and provides insights into its effectiveness in challenging environments. We surveyed state-of-the-art techniques that address corruption robustness, including data augmentation, robust representation learning, knowledge distillation, and robust network layer. As current benchmark results are not obtained in a unified and coherent way, we constructed a benchmark framework that allows for a unified evaluation of corruption robustness in computer vision. Using this framework, we evaluated a few state-of-the-art techniques and popular ImageNet pretrained backbones. Augmentation-based approaches are the currently best approach to improve corruption robustness, and models with transformer architecture exhibit better corruption robustness than CNNs. Large dataset sizes and models improve corruption robustness to some extent but at the cost of more computational resources. However, the degree of improvement in robustness does not always correspond with the size of the models, showing that solely scaling up the models is not sufficient to ensure better corruption robustness. We suggest that future research focus on efficient learning techniques that can work with limited computational resources and data, while also exploring the connection among corruption robustness, OOD generalization, and shortcut learning mitigation to gain deeper insight into the intrinsic mechanism and generalization abilities of models.

## REFERENCES

[1] G. Vishnuvardhan and V. Ravi, "Face recognition using transfer learning on facenet: Application to banking operations," in *Modern Approaches in Machine Learning and Cognitive Science: A Walkthrough: Latest Trends in AI, Volume 2* (V. K. Gunjan and J. M. Zurada, eds.), (Cham), pp. 301–309, Springer International Publishing, 2021.

[2] S. T. Ratnaparkhi, P. Singh, A. Tandasi, and N. Sindhwani, "Comparative analysis of classifiers for criminal identification system using face recognition," in *2021 9th International Conference on Reliability, Infocom Technologies and Optimization (Trends and Future Directions) (ICRITO)*, pp. 1–6, 2021.

[3] L. R. Carlos-Roca, I. H. Torres, and C. F. Tena, "Facial recognition application for border control," in *2018 International Joint Conference on Neural Networks (IJCNN)*, pp. 1–7, 2018.

[4] C. Chen, A. Seff, A. Kornhauser, and J. Xiao, "Deepdriving: Learning affordance for direct perception in autonomous driving," in *2015 IEEE International Conference on Computer Vision (ICCV)*, pp. 2722–2730, 2015.

[5] J. Zhang, X. Wu, and V. S. Sheng, "Learning from crowdsourced labeled data: A survey," *Artificial Intelligence Review*, vol. 46, no. 4, p. 543–576, 2016.

[6] C. Bhatt, I. Kumar, V. Vijayakumar, K. U. Singh, and A. Kumar, "The state of the art of deep learning models in medical science and their challenges," *Multimedia Systems*, vol. 27, no. 4, p. 599–613, 2020.

[7] G. S. Ruthenbeck and K. J. Reynolds, "Virtual reality for medical training: The state-of-the-art," *Journal of Simulation*, vol. 9, no. 1, p. 16–26, 2015.

[8] S. Deniz, D. Lee, G. Kurian, L. Altamirano, D. Yee, M. Ferra, B. Hament, J. Zhan, L. Gewali, and P. Oh, "Computer vision for attendance and emotion analysis in school settings," in *2019 IEEE 9th Annual Computing and Communication Workshop and Conference (CCWC)*, pp. 0134–0139, 2019.

[9] S. Zhang, L. Yao, A. Sun, and Y. Tay, "Deep learning based recommender system: A survey and new perspectives," *ACM Comput. Surv.*, vol. 52, feb 2019.

[10] A. Kumar, "Computer-vision-based fabric defect detection: A survey," *IEEE Transactions on Industrial Electronics*, vol. 55, no. 1, pp. 348–363, 2008.

[11] M. Pak and S. Kim, "A review of deep learning in image recognition," in *2017 4th International Conference on Computer Applications and Information Processing Technology (CAIPT)*, pp. 1–3, 2017.

[12] L. Liu, W. Ouyang, X. Wang, P. Fieguth, J. Chen, X. Liu, and M. Pietikäinen, "Deep learning for generic object detection: A survey," *International Journal of Computer Vision*, vol. 128, pp. 261–318, 2020.

[13] S. Minaee, Y. Boykov, F. Porikli, A. Plaza, N. Kehtarnavaz, and D. Terzopoulos, "Image segmentation using deep learning: A survey," 2020.

[14] M. Stefanini, M. Cornia, L. Baraldi, S. Cascianelli, G. Fiameni, and R. Cucchiara, "From show to tell: A survey on deep learning-based image captioning," 2021.

[15] Z. Wang, J. Chen, and S. C. H. Hoi, "Deep learning for image super-resolution: A survey," 2019.

[16] H. B. Yedder, B. Cardoen, and G. Hamarneh, "Deep learning for biomedical image reconstruction: a survey," *Artificial Intelligence Review*, vol. 54, pp. 215–251, aug 2020.

[17] A. Figueira and B. Vaz, "Survey on synthetic data generation, evaluation methods and gans," *Mathematics*, vol. 10, no. 15, 2022.

[18] S. R. Dubey, "A decade survey of content based image retrieval using deep learning," *IEEE Transactions on Circuits and Systems for Video Technology*, vol. 32, no. 5, pp. 2687–2704, 2022.

[19] Z. Shen, J. Liu, Y. He, X. Zhang, R. Xu, H. Yu, and P. Cui, "Towards out-of-distribution generalization: A survey," 2021.

[20] K.-H. Yu, A. L. Beam, and I. S. Kohane, "Artificial intelligence in healthcare," *Nature Biomedical Engineering*, vol. 2, pp. 719–731, 2018.

[21] R. Geirhos, C. R. M. Temme, J. Rauber, H. H. Schütt, M. Bethge, and F. A. Wichmann, "Generalisation in humans and deep neural networks," vol. 31, Curran Associates, Inc., 2018.

[22] B. Recht, R. Roelofs, L. Schmidt, and V. Shankar, "Do ImageNet classifiers generalize to ImageNet?," in *Proceedings of the 36th International Conference on Machine Learning* (K. Chaudhuri and R. Salakhutdinov, eds.), vol. 97 of *Proceedings of Machine Learning Research*, pp. 5389–5400, PMLR, 09–15 Jun 2019.

[23] B. Frenay and M. Verleysen, "Classification in the presence of label noise: A survey," *IEEE Transactions on Neural Networks and Learning Systems*, vol. 25, no. 5, pp. 845–869, 2014.

[24] R. Geirhos, J.-H. Jacobsen, C. Michaelis, R. Zemel, W. Brendel, M. Bethge, and F. A. Wichmann, "Shortcut learning in deep neural networks," *Nature Machine Intelligence*, vol. 2, pp. 665–673, nov 2020.

[25] X. Zhu and X. Wu, "Class noise vs. attribute noise: A quantitative study," *Artificial Intelligence Review*, vol. 22, no. 3, pp. 177–210, 2004.

[26] G. Algan and I. Ulusoy, "Image classification with deep learning in the presence of noisy labels: A survey," *Knowledge-Based Systems*, vol. 215, p. 106771, Mar 2021.

[27] H. Song, M. Kim, D. Park, and J.-G. Lee, "Learning from noisy labels with deep neural networks: A survey," 2020.

[28] D. Arpit, S. Jastrzkebski, N. Ballas, D. Krueger, E. Bengio, M. S. Kanwal, T. Maharaj, A. Fischer, A. Courville, Y. Bengio, and S. Lacoste-Julien, "A closer look at memorization in deep networks," in *Proceedings of the 34th International Conference on Machine Learning* (D. Precup and Y. W. Teh, eds.), vol. 70 of *Proceedings of Machine Learning Research*, (International Convention Centre, Sydney, Australia), pp. 233–242, PMLR, 06–11 Aug 2017.

[29] C. Zhang, S. Bengio, M. Hardt, B. Recht, and O. Vinyals, "Understanding deep learning requires rethinking generalization," 2017.

[30] S. Lapuschkin, S. Wäldchen, A. Binder, *et al.*, "Unmasking Clever Hans predictors and assessing what machines really learn," *Nat Commun 10*, vol. 1096, 2019.

[31] A. Chakraborty, M. Alam, V. Dey, A. Chattopadhyay, and D. Mukhopadhyay, "Adversarial attacks and defences: A survey," 2018.

[32] D. Hendrycks and T. Dietterich, "Benchmarking neural network robustness to common corruptions and perturbations," *Proceedings of the International Conference on Learning Representations*, 2019.

[33] R. Gao and K. Grauman, "On-demand learning for deep image restoration," in *2017 IEEE International Conference on Computer Vision (ICCV)*, pp. 1095–1104, 2017.

[34] J. Lehtinen, J. Munkberg, J. Hasselgren, S. Laine, T. Karras, M. Aittala, and T. Aila, "Noise2noise: Learning image restoration without clean data," 2018.

[35] A. Krull, T.-O. Buchholz, and F. Jug, "Noise2void - learning denoising from single noisy images," 2019.

[36] J. Xu, Y. Huang, M. M. Cheng, L. Liu, F. Zhu, Z. Xu, and L. Shao, "Noisy-as-clean: Learning self-supervised denoising from corrupted image," *IEEE Transactions on Image Processing*, vol. 29, pp. 9316–9329, 2020.

[37] L. Zhang, M. Yu, T. Chen, Z. Shi, C. Bao, and K. Ma, "Auxiliary training: Towards accurate and robust models," in *Proceedings of the IEEE/CVF Conference on Computer Vision and Pattern Recognition (CVPR)*, June 2020.

[38] D. Hendrycks, N. Mu*, E. D. Cubuk, B. Zoph, J. Gilmer, and B. Lakshminarayanan, "Augmix: A simple method to improve robustness and uncertainty under data shift," in *International Conference on Learning Representations*, 2020.

[39] R. Anirudh, J. J. Thiagarajan, B. Kailkhura, and T. Bremer, "Mimicgan: Robust projection onto image manifolds with corruption mimicking," 2020.

[40] E. Mintun, A. Kirillov, and S. Xie, "On interaction between augmentations and corruptions in natural corruption robustness," 2021.

[41] O. F. Kar, T. Yeo, and A. Zamir, "3d common corruptions for object recognition," in *ICML 2022 Shift Happens Workshop*, 2022.

[42] O. Press, S. Schneider, M. Kuemmerer, and M. Bethge, "CCC: Continuously changing corruptions," in *ICML 2022 Shift Happens Workshop*, 2022.

[43] S. H. Silva and P. Najafirad, "Opportunities and challenges in deep learning adversarial robustness: A survey," 2020.

[44] H. Maennel, I. M. Alabdulmohsin, I. O. Tolstikhin, R. Baldock, O. Bousquet, S. Gelly, and D. Keysers, "What do neural networks learn when trained with random labels?," vol. 33, pp. 19693–19704, Curran Associates, Inc., 2020.

[45] N. Nigam, T. Dutta, and H. P. Gupta, "Impact of noisy labels in learning techniques: A survey," in *Advances in Data and Information Sciences* (M. L. Kolhe, S. Tiwari, M. C. Trivedi, and K. K. Mishra, eds.), (Singapore), pp. 403–411, Springer Singapore, 2020.

[46] F. R. Cordeiro and G. Carneiro, "A survey on deep learning with noisy labels: How to train your model when you cannot trust on the annotations?," 2020.

[47] H. Song, M. Kim, D. Park, Y. Shin, and J.-G. Lee, "Learning from noisy labels with deep neural networks: A survey," 2020.

[48] X. Liu, M. Cheng, H. Zhang, and C.-J. Hsieh, "Towards robust neural networks via random self-ensemble," in *Proceedings of the European Conference on Computer Vision (ECCV)*, September 2018.

[49] I. Goodfellow, J. Shlens, and C. Szegedy, "Explaining and harnessing adversarial examples," in *International Conference on Learning Representations*, 2015.

[50] S. Gu and L. Rigazio, "Towards deep neural network architectures robust to adversarial examples," 2014.

[51] T. Pang, C. Du, Y. Dong, and J. Zhu, "Towards ro-

bust detection of adversarial examples," in *Advances in Neural Information Processing Systems* (S. Bengio, H. Wallach, H. Larochelle, K. Grauman, N. Cesa-Bianchi, and R. Garnett, eds.), vol. 31, Curran Associates, Inc., 2018.

[52] K. Kireev, M. Andriushchenko, and N. Flammarion, "On the effectiveness of adversarial training against common corruptions," 2021.

[53] A. Kuznetsova, H. Rom, N. Alldrin, J. Uijlings, I. Krasin, J. Pont-Tuset, S. Kamali, S. Popov, M. Malloci, A. Kolesnikov, T. Duerig, and V. Ferrari, "The open images dataset v4," *International Journal of Computer Vision*, vol. 128, pp. 1956–1981, mar 2020.

[54] J. C. Chang, S. Amershi, and E. Kamar, "Revolt: Collaborative crowdsourcing for labeling machine learning datasets," in *Proceedings of the 2017 CHI Conference on Human Factors in Computing Systems*, CHI '17, (New York, NY, USA), p. 2334–2346, Association for Computing Machinery, 2017.

[55] J. Zhang, X. Wu, and V. S. Sheng, "Learning from crowdsourced labeled data: a survey," *Artificial Intelligence Review*, vol. 46, pp. 543–576, 2016.

[56] L. Jing and Y. Tian, "Self-supervised visual feature learning with deep neural networks: A survey," *IEEE Transactions on Pattern Analysis and Machine Intelligence*, vol. 43, no. 11, pp. 4037–4058, 2021.

[57] J. Muhammadi, H. R. Rabiee, and A. Hosseini, "Crowd labeling: a survey," 2013.

[58] B. Han, Q. Yao, T. Liu, G. Niu, I. W. Tsang, J. T. Kwok, and M. Sugiyama, "A survey of label-noise representation learning: Past, present and future," 2020.

[59] E. Rusak, S. Schneider, G. Pachitariu, L. Eck, P. Gehler, O. Bringmann, W. Brendel, and M. Bethge, "If your data distribution shifts, use self-learning," 2021.

[60] T. Salvador and A. M. Oberman, "Imagenet-cartoon and imagenet-drawing: two domain shift datasets for imagenet," in *ICML 2022 Shift Happens Workshop*, 2022.

[61] D. Hendrycks, S. Basart, N. Mu, S. Kadavath, F. Wang, E. Dorundo, R. Desai, T. Zhu, S. Parajuli, M. Guo, D. Song, J. Steinhardt, and J. Gilmer, "The many faces of robustness: A critical analysis of out-of-distribution generalization," in *Proceedings of the IEEE/CVF International Conference on Computer Vision (ICCV)*, pp. 8340–8349, October 2021.

[62] D. Hendrycks, K. Zhao, S. Basart, J. Steinhardt, and D. Song, "Natural adversarial examples," *CVPR*, 2021.

[63] M. Pintor, D. Angioni, A. Sotgiu, L. Demetrio, A. Demontis, B. Biggio, and F. Roli, "Imagenet-patch: A dataset for benchmarking machine learning robustness against adversarial patches," 2022.

[64] B. Zhao, S. Yu, W. Ma, M. Yu, S. Mei, A. Wang, J. He, A. Yuille, and A. Kortylewski, "Ood-cv: A benchmark for robustness to out-of-distribution shifts of individual nuisances in natural images," 2021.

[65] J. Yung, R. Romijnders, A. Kolesnikov, L. Beyer, J. Djolonga, N. Houlsby, S. Gelly, M. Lucic, and X. Zhai, "SI-score: An image dataset for fine-grained analysis of robustness to object location, rotation and size," in *ICML 2022 Shift Happens Workshop*, 2022.

[66] P. W. Koh, S. Sagawa, H. Marklund, S. M. Xie, M. Zhang, A. Balsubramani, W. Hu, M. Yasunaga, R. L. Phillips, I. Gao, T. Lee, E. David, I. Stavness, W. Guo, B. A. Earnshaw, I. S. Haque, S. Beery, J. Leskovec, A. Kundaje, E. Pierson, S. Levine, C. Finn, and P. Liang, "Wilds: A benchmark of in-the-wild distribution shifts," 2020.

[67] R. Taori, A. Dave, V. Shankar, N. Carlini, B. Recht, and L. Schmidt, "Measuring robustness to natural distribution shifts in image classification," 2020.

[68] C. Guo, G. Pleiss, Y. Sun, and K. Q. Weinberger, "On calibration of modern neural networks," 2017.

[69] Q. Xie, M. T. Luong, E. Hovy, and Q. V. Le, "Self-training with noisy student improves imagenet classification," in *2020 IEEE/CVF Conference on Computer Vision and Pattern Recognition (CVPR)*, pp. 10684–10695, 2020.

[70] A. Robey, H. Hassani, and G. J. Pappas, "Model-based robust deep learning: Generalizing to natural, out-of-distribution data," 2020.

[71] C. Shorten and T. M. Khoshgoftaar, "A survey on image data augmentation for deep learning," *Journal of Big Data*, vol. 6, no. 1, p. 60, 2019.

[72] G. Kang, X. Dong, L. Zheng, and Y. Yang, "Patchshuffle regularization," 2017.

[73] Z. Zhong, L. Zheng, G. Kang, S. Li, and Y. Yang, "Random erasing data augmentation," 2017.

[74] R. G. Lopes, D. Yin, B. Poole, J. Gilmer, and E. D. Cubuk, "Improving robustness without sacrificing accuracy with patch gaussian augmentation," 2019.

[75] H. Zhang, M. Cisse, Y. N. Dauphin, and D. Lopez-Paz, "mixup: Beyond empirical risk minimization," 2017.

[76] J. Ngnawé, M. NJIFON, J. Heek, and Y. Dauphin, "Robustmix: Improving robustness by regularizing the frequency bias of deep nets," 2022.

[77] H. Wang, X. Wu, Z. Huang, and E. P. Xing, "High frequency component helps explain the generalization of convolutional neural networks," 2020.

[78] R. Geirhos, P. Rubisch, C. Michaelis, M. Bethge, F. A. Wichmann, and W. Brendel, "Imagenet-trained CNNs are biased towards texture; increasing shape bias improves accuracy and robustness.," in *International Conference on Learning Representations*, 2019.

[79] H. Yao, Y. Wang, S. Li, L. Zhang, W. Liang, J. Zou, and C. Finn, "Improving out-of-distribution robustness via selective augmentation," in *Proceedings of the 39th International Conference on Machine Learning* (K. Chaudhuri, S. Jegelka, L. Song, C. Szepesvari, G. Niu, and S. Sabato, eds.), vol. 162 of *Proceedings of Machine Learning Research*, pp. 25407–25437, PMLR, 17–23 Jul 2022.

[80] E. D. Cubuk, B. Zoph, D. Mane, V. Vasudevan, and Q. V. Le, "Autoaugment: Learning augmentation policies from data," 2019.

[81] R. Soklaski, M. Yee, and T. Tsiligkaridis, "Fourier-based augmentations for improved robustness and uncertainty calibration," 2022.

[82] H. Wang, C. Xiao, J. Kossaifi, Z. Yu, A. Anandkumar, and Z. Wang, "Augmax: Adversarial composition of random augmentations for robust training," 2021.

[83] A. Modas, R. Rade, G. Ortiz-Jiménez, S.-M. Moosavi-Dezfooli, and P. Frossard, "Prime: A few primitives can boost robustness to common corruptions," 2021.

[84] I. Kim, Y. Kim, and S. Kim, "Learning loss for test-time augmentation," in *Advances in Neural Information Processing Systems* (H. Larochelle, M. Ranzato, R. Hadsell, M. Balcan, and H. Lin, eds.), vol. 33, pp. 4163–4174, Curran Associates, Inc., 2020.

[85] I. Gao, S. Sagawa, P. W. Koh, T. Hashimoto, and P. Liang, "Out-of-distribution robustness via targeted augmentations," in *NeurIPS 2022 Workshop on Distribution Shifts: Connecting Methods and Applications*, 2022.

[86] T. Karras, S. Laine, and T. Aila, "A style-based generator architecture for generative adversarial networks," 2019.

[87] G. G. Chrysos, J. Kossaifi, and S. Zafeiriou, "Rocgan: Robust conditional gan," *International Journal of Computer Vision*, vol. 128, no. 10, pp. 2665–2683, 2020.

[88] M. Mirza and S. Osindero, "Conditional generative adversarial nets," 2014.

[89] J.-Y. Zhu, T. Park, P. Isola, and A. A. Efros, "Unpaired image-to-image translation using cycle-consistent adversarial networks," in *Computer Vision (ICCV), 2017 IEEE International Conference on*, 2017.

[90] J. P. Yun, W. C. Shin, G. Koo, M. S. Kim, C. Lee, and S. J. Lee, "Automated defect inspection system for metal surfaces based on deep learning and data augmentation," *Journal of Manufacturing Systems*, vol. 55, pp. 317–324, 2020.

[91] M. Hammami, D. Friboulet, and R. Kechichian, "Cycle gan-based data augmentation for multi-organ detection in ct images via yolo," in *2020 IEEE International Conference on Image Processing (ICIP)*, pp. 390–393, 2020.

[92] Z. Xu, C. Qi, and G. Xu, "Semi-supervised attention-guided cyclegan for data augmentation on medical images," in *2019 IEEE International Conference on Bioinformatics and Biomedicine (BIBM)*, pp. 563–568, 2019.

[93] C. Yi, H. Li, R. Wan, and A. C. Kot, "Improving robustness of dnns against common corruptions via gaussian adversarial training," in *2020 IEEE International Conference on Visual Communications and Image Processing (VCIP)*, pp. 17–20, 2020.

[94] A. Madry, A. Makelov, L. Schmidt, D. Tsipras, and A. Vladu, "Towards deep learning models resistant to adversarial attacks," in *International Conference on Learning Representations*, 2018.

[95] C. Guo, M. Lee, G. Leclerc, J. Dapello, Y. Rao, A. Madry, and J. Dicarlo, "Adversarially trained neural representations are already as robust as biological neural representations," in *Proceedings of the 39th International Conference on Machine Learning* (K. Chaudhuri, S. Jegelka, L. Song, C. Szepesvari, G. Niu, and S. Sabato, eds.), vol. 162 of *Proceedings of Machine Learning Research*, pp. 8072–8081, PMLR, 17–23 Jul 2022.

[96] D. A. Calian, F. Stimberg, O. Wiles, S.-A. Rebuffi, A. Gyorgy, T. Mann, and S. Gowal, "Defending against image corruptions through adversarial augmentations," 2021.

[97] L. Zhao, T. Liu, X. Peng, and D. Metaxas, "Maximum-entropy adversarial data augmentation for improved generalization and robustness," 2020.

[98] A. S. Liu, X. L. Liu, H. Yu, C. Z. Zhang, Q. Liu, and D. C. Tao, "Training robust deep neural networks via adversarial noise propagation," *IEEE TRANSACTIONS ON IMAGE PROCESSING*, vol. 30, pp. 5769–5781, 2021.

[99] N. B. Erichson, S. H. Lim, W. Xu, F. Utrera, Z. Cao, and M. W. Mahoney, "Noisymix: Boosting model robustness to common corruptions," 2022.

[100] S. Addepalli, S. Jain, and R. V. Babu, "Efficient and effective augmentation strategy for adversarial training," 2022.

[101] T. Chen, S. Kornblith, M. Norouzi, and G. Hinton, "A simple framework for contrastive learning of visual representations," in *Proceedings of the 37th International Conference on Machine Learning* (H. D. III and A. Singh, eds.), vol. 119 of *Proceedings of Machine Learning Research*, pp. 1597–1607, PMLR, 13–18 Jul 2020.

[102] P. Khosla, P. Teterwak, C. Wang, A. Sarna, Y. Tian, P. Isola, A. Maschinot, C. Liu, and D. Krishnan, "Supervised contrastive learning," 2021.

[103] W. Du, H. Chen, and H. Yang, "Learning invariant representation for unsupervised image restoration," 2020.

[104] D. Hendrycks, M. Mazeika, S. Kadavath, and D. Song, "Using self-supervised learning can improve model robustness and uncertainty," 2019.

[105] T. Chen, S. Kornblith, M. Norouzi, and G. Hinton, "A simple framework for contrastive learning of visual representations," 2020.

[106] S. A. Taghanaki, K. Choi, A. Khasahmadi, and A. Goyal, "Robust representation learning via perceptual similarity metrics," 2021.

[107] Z. Jiang, T. Chen, T. Chen, and Z. Wang, "Robust pre-training by adversarial contrastive learning," in *Advances in Neural Information Processing Systems* (H. Larochelle, M. Ranzato, R. Hadsell, M. Balcan, and H. Lin, eds.), vol. 33, pp. 16199–16210, Curran Associates, Inc., 2020.

[108] S. Chakraborty, A. R. Gosthipaty, and S. Paul, "G-simclr : Self-supervised contrastive learning with guided projection via pseudo labelling," 2020.

[109] M. Chen, D. Y. Fu, A. Narayan, M. Zhang, Z. Song, K. Fatahalian, and C. Re, "Perfectly balanced: Improving transfer and robustness of supervised contrastive learning," in *Proceedings of the 39th International Conference on Machine Learning* (K. Chaudhuri, S. Jegelka, L. Song, C. Szepesvari, G. Niu, and S. Sabato, eds.), vol. 162 of *Proceedings of Machine Learning Research*, pp. 3090–3122, PMLR, 17–23 Jul 2022.

[110] A. van den Oord, Y. Li, and O. Vinyals, "Representation learning with contrastive predictive coding," 2019.

[111] M. Zhang, N. S. Sohoni, H. R. Zhang, C. Finn, and C. Re, "Correct-n-contrast: a contrastive approach for improving robustness to spurious correlations," in *Proceedings of the 39th International Conference on Machine Learning* (K. Chaudhuri, S. Jegelka, L. Song, C. Szepesvari, G. Niu, and S. Sabato, eds.), vol. 162 of *Proceedings of Machine Learning Research*, pp. 26484–26516, PMLR, 17–23 Jul 2022.

[112] S. Laine, T. Karras, J. Lehtinen, and T. Aila, "High-quality self-supervised deep image denoising," 2019.

[113] S. Ioffe and C. Szegedy, "Batch normalization: Accelerating deep network training by reducing internal covariate shift," 2015.

[114] Y. Wu and K. He, "Group normalization," in *Proceedings of the European Conference on Computer Vision (ECCV)*, September 2018.

[115] D. Ulyanov, A. Vedaldi, and V. Lempitsky, "Instance normalization: The missing ingredient for fast stylization," 2017.

[116] N. Strisciuglio, M. Lopez-Antequera, and N. Petkov, "Enhanced robustness of convolutional networks with a push–pull inhibition layer," *Neural Computing and Applications*, vol. 32, no. 24, pp. 17957–17971, 2020.

[117] N. Strisciuglio and G. Azzopardi, "Visual response inhibition for increased robustness of convolutional networks to distribution shifts," in *NeurIPS 2022 Workshop on Distribution Shifts: Connecting Methods and Applications*, 2022.

[118] Z. Babaiee, R. Hasani, M. Lechner, D. Rus, and R. Grosu, "On-off center-surround receptive fields for accurate and robust image classification," 2021.

[119] N. Park and S. Kim, "Blurs behave like ensembles: Spatial smoothings to improve accuracy, uncertainty, and robustness," in *Proceedings of the 39th International Conference on Machine Learning* (K. Chaudhuri, S. Jegelka, L. Song, C. Szepesvari, G. Niu, and S. Sabato, eds.), vol. 162 of *Proceedings of Machine Learning Research*, pp. 17390–17419, PMLR, 17–23 Jul 2022.

[120] J. Diffenderfer, B. R. Bartoldson, S. Chaganti, J. Zhang, and B. Kailkhura, "A winning hand: Compressing deep networks can improve out-of-distribution robustness," 2021.

[121] T. Chen, Z. Zhang, S. Liu, Y. Zhang, S. Chang, and Z. Wang, "Data-efficient double-win lottery tickets from robust pre-training," in *Proceedings of the 39th International Conference on Machine Learning* (K. Chaudhuri, S. Jegelka, L. Song, C. Szepesvari, G. Niu, and S. Sabato, eds.), vol. 162 of *Proceedings of Machine Learning Research*, pp. 3747–3759, PMLR, 17–23 Jul 2022.

[122] M. Teti, G. Kenyon, B. Migliori, and J. Moore, "LCANets: Lateral competition improves robustness against corruption and attack," in *Proceedings of the 39th International Conference on Machine Learning* (K. Chaudhuri, S. Jegelka, L. Song, C. Szepesvari, G. Niu, and S. Sabato, eds.), vol. 162 of *Proceedings of Machine Learning Research*, pp. 21232–21252, PMLR, 17–23 Jul 2022.

[123] P. Benz, C. Zhang, and I. S. Kweon, "Batch normalization increases adversarial vulnerability: Disentangling usefulness and robustness of model features," 2020.

[124] P. Benz, C. Zhang, A. Karjauv, and I. S. Kweon, "Revisiting batch normalization for improving corruption robustness," 2021.

[125] W.-G. Chang, T. You, S. Seo, S. Kwak, and B. Han, "Domain-specific batch normalization for unsupervised domain adaptation," 2019.

[126] Y. Li, N. Wang, J. Shi, J. Liu, and X. Hou, "Revisiting batch normalization for practical domain adaptation," 2016.

[127] Z. Xu, X. Yang, X. Li, and X. Sun, "The effectiveness of instance normalization: a strong baseline for single image dehazing," 2018.

[128] S. Liu, X. Li, Y. Zhai, C. You, Z. Zhu, C. Fernandez-Granda, and Q. Qu, "Convolutional normalization: Improving deep convolutional network robustness and training," 2022.

[129] L. Zhao, T. Liu, X. Peng, and D. Metaxas, "Maximum-entropy adversarial data augmentation for improved generalization and robustness," in *Advances in Neural Information Processing Systems* (H. Larochelle, M. Ranzato, R. Hadsell, M. Balcan, and H. Lin, eds.), vol. 33, pp. 14435–14447, Curran Associates, Inc., 2020.

[130] K. He, X. Zhang, S. Ren, and J. Sun, "Deep residual learning for image recognition," 2015.

[131] S. Zagoruyko and N. Komodakis, "Wide residual networks," 2017.

[132] S. Xie, R. Girshick, P. Dollár, Z. Tu, and K. He, "Aggregated residual transformations for deep neural networks," 2017.

[133] G. Huang, Z. Liu, L. van der Maaten, and K. Q. Weinberger, "Densely connected convolutional networks," 2018.

[134] M. Tan and Q. V. Le, "Efficientnet: Rethinking model scaling for convolutional neural networks," 2020.

[135] Z. Dai, H. Liu, Q. V. Le, and M. Tan, "Coatnet: Marrying convolution and attention for all data sizes," 2021.

[136] Z. Liu, H. Mao, C.-Y. Wu, C. Feichtenhofer, T. Darrell, and S. Xie, "A convnet for the 2020s," 2022.

[137] A. Kolesnikov, L. Beyer, X. Zhai, J. Puigcerver, J. Yung, S. Gelly, and N. Houlsby, "Big transfer (bit): General visual representation learning," 2020.

[138] Z. Liu, Y. Lin, Y. Cao, H. Hu, Y. Wei, Z. Zhang, S. Lin, and B. Guo, "Swin transformer: Hierarchical vision transformer using shifted windows," 2021.

[139] L. Yuan, Q. Hou, Z. Jiang, J. Feng, and S. Yan, "Volo: Vision outlooker for visual recognition," 2021.

[140] A. Dosovitskiy, L. Beyer, A. Kolesnikov, D. Weissenborn, X. Zhai, T. Unterthiner, M. Dehghani, M. Minderer, G. Heigold, S. Gelly, J. Uszkoreit, and N. Houlsby, "An image is worth 16x16 words: Transformers for image recognition at scale," 2021.

[141] H. Bao, L. Dong, S. Piao, and F. Wei, "Beit: Bert pre-training of image transformers," 2022.

[142] M. Maaz, A. Shaker, H. Cholakkal, S. Khan, S. W. Zamir, R. M. Anwer, and F. S. Khan, "Edgenext: Efficiently amalgamated cnn-transformer architecture for mobile vision applications," 2022.

[143] Y. Li, C.-Y. Wu, H. Fan, K. Mangalam, B. Xiong, J. Malik, and C. Feichtenhofer, "Mvitv2: Improved multiscale vision transformers for classification and detection," 2022.

[144] Z. Tu, H. Talebi, H. Zhang, F. Yang, P. Milanfar, A. Bovik, and Y. Li, "Maxvit: Multi-axis vision transformer," 2022.

[145] S. Lefkimmiatis, "Universal denoising networks : A novel cnn architecture for image denoising," in *2018 IEEE/CVF Conference on Computer Vision and Pattern Recognition*, pp. 3204–3213, 2018.

[146] X. Glorot, A. Bordes, and Y. Bengio, "Deep sparse rectifier neural networks," in *Proceedings of the Fourteenth*

*International Conference on Artificial Intelligence and Statistics* (G. Gordon, D. Dunson, and M. Dudík, eds.), vol. 15 of *Proceedings of Machine Learning Research*, (Fort Lauderdale, FL, USA), pp. 315–323, PMLR, 11–13 Apr 2011.

[147] A. Krogh and J. Hertz, "A simple weight decay can improve generalization," in *Advances in Neural Information Processing Systems* (J. Moody, S. Hanson, and R. Lippmann, eds.), vol. 4, Morgan-Kaufmann, 1991.

[148] N. Srivastava, G. Hinton, A. Krizhevsky, I. Sutskever, and R. Salakhutdinov, "Dropout: A simple way to prevent neural networks from overfitting," *Journal of Machine Learning Research*, vol. 15, no. 56, pp. 1929–1958, 2014.

[149] C. Blundell, J. Cornebise, K. Kavukcuoglu, and D. Wierstra, "Weight uncertainty in neural network," in *Proceedings of the 32nd International Conference on Machine Learning* (F. Bach and D. Blei, eds.), vol. 37 of *Proceedings of Machine Learning Research*, (Lille, France), pp. 1613–1622, PMLR, 07–09 Jul 2015.

[150] G. Pereyra, G. Tucker, J. Chorowski, Łukasz Kaiser, and G. Hinton, "Regularizing neural networks by penalizing confident output distributions," 2017.

[151] H. Wang, S. Ge, E. P. Xing, and Z. C. Lipton, "Learning robust global representations by penalizing local predictive power," 2019.

[152] C. E. R. K. Lassance, V. Gripon, and A. Ortega, "Laplacian networks: Bounding indicator function smoothness for neural network robustness," 2018.

[153] T. Tulabandhula and C. Rudin, "Robust optimization using machine learning for uncertainty sets," 2014.

[154] S. Sagawa, P. W. Koh, T. B. Hashimoto, and P. Liang, "Distributionally robust neural networks for group shifts: On the importance of regularization for worst-case generalization," 2020.

[155] D. Bertsimas, V. Gupta, and N. Kallus, "Data-driven robust optimization," 2014.

[156] A. Setlur, D. Dennis, B. Eysenbach, A. Raghunathan, C. Finn, V. Smith, and S. Levine, "Bitrate-constrained DRO: Beyond worst case robustness to unknown group shifts," in *NeurIPS 2022 Workshop on Distribution Shifts: Connecting Methods and Applications*, 2022.

[157] S. S. Tay, C. S. Foo, U. Daisuke, R. Leong, and B. K. H. Low, "Efficient distributionally robust Bayesian optimization with worst-case sensitivity," in *Proceedings of the 39th International Conference on Machine Learning* (K. Chaudhuri, S. Jegelka, L. Song, C. Szepesvari, G. Niu, and S. Sabato, eds.), vol. 162 of *Proceedings of Machine Learning Research*, pp. 21180–21204, PMLR, 17–23 Jul 2022.

[158] S. Chang, Y. Zhang, M. Yu, and T. S. Jaakkola, "Invariant rationalization," 2020.

[159] M. Koyama and S. Yamaguchi, "When is invariance useful in an out-of-distribution generalization problem ?," 2021.

[160] N. Mehrabi, F. Morstatter, N. Saxena, K. Lerman, and A. Galstyan, "A survey on bias and fairness in machine learning," *ACM Comput. Surv.*, vol. 54, jul 2021.

[161] M. Nauta, R. Walsh, A. Dubowski, and C. Seifert, "Uncovering and correcting shortcut learning in machine learning models for skin cancer diagnosis," *Diagnostics*, vol. 12, no. 1, 2022.

[162] S. Wang, R. Veldhuis, C. Brune, and N. Strisciuglio, "Frequency shortcut learning in neural networks," in *NeurIPS 2022 Workshop on Distribution Shifts: Connecting Methods and Applications*, 2022.

[163] M. Pezeshki, S.-O. Kaba, Y. Bengio, A. Courville, D. Precup, and G. Lajoie, "Gradient starvation: A learning proclivity in neural networks," in *Advances in Neural Information Processing Systems* (A. Beygelzimer, Y. Dauphin, P. Liang, and J. W. Vaughan, eds.), 2021.

[164] M. Du, V. Manjunatha, R. Jain, R. Deshpande, F. Dernoncourt, J. Gu, T. Sun, and X. Hu, "Towards interpreting and mitigating shortcut learning behavior of nlu models," 2021.

[165] N. Dagaev, B. D. Roads, X. Luo, D. N. Barry, K. R. Patil, and B. C. Love, "A too-good-to-be-true prior to reduce shortcut reliance," 2021.

[166] S. Ahn, S. Kim, and S.-Y. Yun, "Mitigating dataset bias by using per-sample gradient," in *NeurIPS 2022 Workshop on Distribution Shifts: Connecting Methods and Applications*, 2022.

[167] M. Minderer, O. Bachem, N. Houlsby, and M. Tschannen, "Automatic shortcut removal for self-supervised representation learning," 2020.

[168] J. Robinson, L. Sun, K. Yu, K. Batmanghelich, S. Jegelka, and S. Sra, "Can contrastive learning avoid shortcut solutions?," 2021.

[169] K. He, H. Fan, Y. Wu, S. Xie, and R. Girshick, "Momentum contrast for unsupervised visual representation learning," 2019.

[170] F. Zhuang, Z. Qi, K. Duan, D. Xi, Y. Zhu, H. Zhu, H. Xiong, and Q. He, "A comprehensive survey on transfer learning," 2020.

[171] T. Hospedales, A. Antoniou, P. Micaelli, and A. Storkey, "Meta-learning in neural networks: A survey," 2020.

[172] Y. Song, T. Wang, S. K. Mondal, and J. P. Sahoo, "A comprehensive survey of few-shot learning: Evolution, applications, challenges, and opportunities," 2022.

[173] H. Shah, K. Tamuly, A. Raghunathan, P. Jain, and P. Netrapalli, "The pitfalls of simplicity bias in neural networks," 2020.

[174] P. Izmailov, P. Kirichenko, N. Gruver, and A. G. Wilson, "On feature learning in the presence of spurious correlations," in *Advances in Neural Information Processing Systems* (S. Koyejo, S. Mohamed, A. Agarwal, D. Belgrave, K. Cho, and A. Oh, eds.), vol. 35, pp. 38516–38532, Curran Associates, Inc., 2022.

[175] R. Xu, X. Zhang, Z. Shen, T. Zhang, and P. Cui, "A theoretical analysis on independence-driven importance weighting for covariate-shift generalization," 2022.

[176] A. Goyal and Y. Bengio, "Inductive biases for deep learning of higher-level cognition," *Proceedings of the Royal Society A: Mathematical, Physical and Engineering Sciences*, vol. 478, no. 2266, p. 20210068, 2022.